Is It Homogeneous or Heterogeneous Catalysis Derived from [RhCp*Cl$_2$]$_2$? *In Operando* XAFS, Kinetic, and Crucial Kinetic Poisoning Evidence for Subnanometer Rh$_4$ Cluster-Based Benzene Hydrogenation Catalysis

Ercan Bayram,[†] John C. Linehan,*,[‡] John L. Fulton,[‡] John A. S. Roberts,[‡] Nathaniel K. Szymczak,[§] Tricia D. Smurthwaite,[‡] Saim Özkar,[‖] Mahalingam Balasubramanian,[⊥] and Richard G. Finke*,[†]

[†]Department of Chemistry, Colorado State University, Fort Collins, Colorado 80523, United States

[‡]Pacific Northwest National Laboratory, Richland, Washington 99352, United States

[§]Department of Chemistry, University of Michigan, 930 North University Avenue, Ann Arbor, Michigan 48109, United States

[‖]Department of Chemistry, Middle East Technical University, 06531 Ankara Turkey

[⊥]Advanced Photon Source, Argonne National Laboratory, Argonne, Illinois 60439, United States

S *Supporting Information*

ABSTRACT: Determining the true, kinetically dominant catalytically active species, in the classic benzene hydrogenation system pioneered by Maitlis and co-workers 34 years ago starting with [RhCp*Cl$_2$]$_2$ (Cp* = [η^5-C$_5$(CH$_3$)$_5$]), has proven to be one of the most challenging case studies in the quest to distinguish single-metal-based "homogeneous" from polymetallic, "heterogeneous" catalysis. The reason, this study will show, is the previous failure to use the proper combination of: (i) *in operando* spectroscopy to determine the dominant form(s) of the precatalyst's mass under catalysis (i.e., operating) conditions, and then crucially also (ii) the previous lack of the necessary kinetic studies, catalysis being a "wholly kinetic phenomenon" as J. Halpern long ago noted. An important contribution from this study will be to reveal the power of quantitiative kinetic poisoning experiments for distinguishing single-metal, or in the present case subnanometer Rh$_4$ cluster-based catalysis, from larger, polymetallic Rh(0)$_n$ nanoparticle catalysis, at least under favorable conditions. The combined *in operando* X-ray absorption fine structure (XAFS) spectroscopy and kinetic evidence provide a compelling case for Rh$_4$-based, with average stoichiometry "Rh$_4$Cp*$_{2.4}$Cl$_4$H$_c$", benzene hydrogenation catalysis in 2-propanol with added Et$_3$N and at 100 °C and 50 atm initial H$_2$ pressure. The results also reveal, however, that if even ca. 1.4% of the total soluble Rh(0)$_n$ had formed nanoparticles, then those Rh(0)$_n$ nanoparticles would have been able to account for all the observed benzene hydrogenation catalytic rate (using commercial, ca. 2 nm, polyethyleneglycol-dodecylether hydrosol stabilized Rh(0)$_n$ nanoparticles as a model system). The results—especially the poisoning methodology developed and employed—are of significant, broader interest since determining the nature of the true catalyst continues to be a central, often vexing issue in any and all catalytic reactions. The results are also of fundamental interest in that they add to a growing body of evidence indicating that certain, appropriately ligated, coordinatively unsaturated, subnanometer M$_4$ transition-metal clusters can be relatively robust catalysts. Also demonstrated herein is that Rh$_4$ clusters are poisoned by Hg(0), demonstrating for the first time that the classic Hg(0) poisoning test of "homogeneous" vs "heterogeneous" catalysts cannot distinguish Rh$_4$-based subnanometer catalysts from Rh(0)$_n$ nanoparticle catalysts, at least for the present examples of these two specific, Rh-based catalysts.
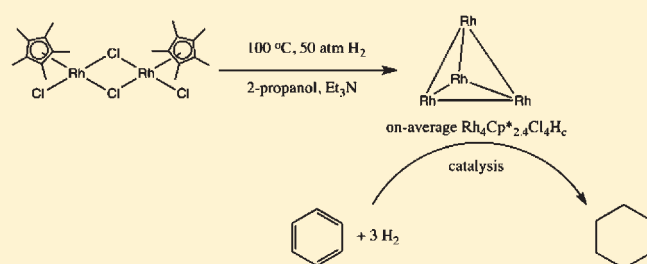
INTRODUCTION

Distinguishing catalysis by a discrete metal complex "homogeneous" catalyst from a multiple metal "heterogeneous" nanoparticle catalyst[1] remains a challenging problem in catalytic science.[2,3] It is also a forefront topic in catalysis since key catalytic properties—including selectivity, activity, stability, catalytic lifetime, and poisoning as well as catalyst recovery and regeneration—are inherently different for homogeneous and heterogeneous catalysts.[2] The problem of the "identification of the true catalyst" is made more intriguing as well as compounded in complexity by the recent findings that subnanometer clusters, such as M$_4$ species, can be active catalysts.[4−7]

Those of us at Colorado State University (CSU) entered the arena of "is it homogeneous or heterogeneous catalysis?" in the pre-1990s with the then generally unsolved problem of how to best and most efficiently approach distinguishing these two types of catalysis; work that resulted in the discovery of polyoxoanion-stabilized

Scheme 1. An Updated Approach to Distinguish Single-Metal Homogeneous Catalysis from Polymetallic Heterogeneous Catalysis (reprinted with permission)[11]
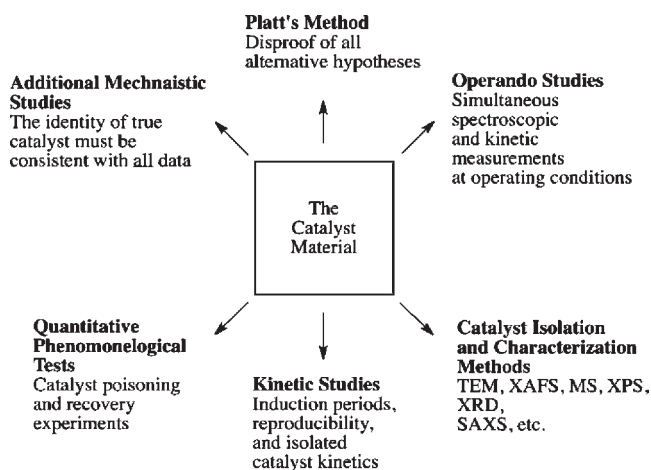
Ir(0)$_n$ nanoparticles[8,9]—plus a more general approach than was available in 1994 for distinguishing homogeneous vs heterogeneous catalysts.[8] At its most basic level, the underlying conceptual basis[10] of that 1994 approach is still the essence of the required approach today: (i) determining where the precatalyst mass resides during catalysis (i.e., in what species or forms) and then necessarily (ii) performing kinetic studies—including quantitative catalyst poisoning studies as the present work will make apparent—since "catalysis is a wholly kinetic phenomenon",[10] at least when starting from favorable reaction thermodynamics. The 1994 methodology, developed via third-row transition metals that tend to form TEM-beam stable nanoparticles (from third-row metal precatalysts that are also often TEM-beam stable), has been updated recently[6,11] by the addition of *in operando*[12] spectroscopic studies that are required for a detailed, correct picture of "what is the evolved form(s) the precatalyst mass" under operating conditions, Scheme 1. Other notable parts of Scheme 1 include: (i) a necessary focus throughout the research on the disproof of multiple alternative hypotheses,[13] (ii) the idea that no single experiment can convincingly determine the true nature of the catalyst,[2,14,15] and again (iii) the required kinetic studies. Although already part of Scheme 1 since 1994,[8] the present work reveals clearly (iv) the power of quantitative kinetic poisoning experiments[2,14,16,17] for distinguishing nanoparticle catalysts (where only a fraction of the total metal atoms in a nanoparticle are on the surface, resulting in poison/M ratios <1) from single metal or M$_4$ catalysts (where 1 or more equivs of poison are expected to be required, poison/M ratios >1). Another key part of Scheme 1 is (v) that the correct description of the catalyst should be able to explain all observations and have predictive value. Aiding the experimental distinction of homogeneous vs nanoparticle heterogeneous catalysts is the early review of that topic in 2003 by one of our groups[2] and a series of subsequent reviews probing the nature of the true palladium catalysts employed for Heck,[18−21] Suzuki,[18] C−C coupling,[22] and hydrogenation[22] reactions.

Also relevant to the present study is the literature of arene hydrogenation,[2,14,23] including the issue of homogeneous vs heterogeneous catalysis therein;[2,14] arene reduction being a topic important to industry.[24] Interesting historically here is that benzene reduction was originally interpreted as a "telltale sign"[14]

of heterogeneous catalysis, benzene hydrogenation often requiring harsher reaction conditions of ≥ 100 °C and ≥ 50 atm.[25]

A now classic "is it homogeneous or heterogeneous catalysis?" problem, identified in our 2003 review,[2] is Maitlis and co-workers' pioneering study of benzene hydrogenation catalysis beginning with [RhCp*Cl$_2$]$_2$ at 50 °C and 50 atm H$_2$ pressure.[26] In 1977 the catalytically active species was suggested to be homogeneous on the basis of a light-scattering experiment—showing the absence of metal particles—and the apparent[27] lack of an observable metal precipitate at the end of the reaction. However, the light-scattering results appeared to depend on the reaction vessel, and small amounts of metal precipitate were occasionally observed (see the Supporting Information elsewhere[27] for additional details and discussion of the early light-scattering experiments). In addition, other authors reported the formation of dark-colored reaction solution and 1−2 h induction periods and the formation of metallic precipitates using this same (pre)-catalyst under the same conditions (i.e., 50 °C and 50 atm H$_2$ pressure).[28] Unfortunately, no kinetic studies were reported as part of the 1977 work,[26] meaning that the true benzene reduction catalyst has remained unknown since that time.[26]

Also relevant to what follows is the report that green colored solutions of [RhCp*H]$_4$[X]$_2$ (where X: Cl, PF$_6$, BF$_4$) are "relatively poor hydrogenation catalysts"[29] in organic solvents, such as acetone or alcohols, due apparently to a high degree of steric shielding of the Rh centers by the Cp* ligands.[29] In short, identifying the benzene hydrogenation catalysis when beginning with [RhCp*Cl$_2$]$_2$ has remained as a significant, central mechanistic challenge to the more general problem of "is it homogeneous or heterogeneous catalysis?"

In 2003, the Colorado State subgroup of our team recognized this challenge[2] and began reinvestigations of the catalytically active species in benzene reduction[27] at 50 atm H$_2$ beginning with [RhCp*Cl$_2$]$_2$ but at 100 °C where more convenient rates are present. (The reduction of benzene at 50 °C beginning with [RhCp*Cl$_2$]$_2$ takes ∼21 days to go to completion, while at 100 °C, the reaction is completed in a much more convenient, ≥ 80-fold faster, ∼6 h period.) A 2005 paper resulted from that work demonstrating an induction period and overall sigmoidal kinetics (see Figure 3 in that 2005 paper[27]), kinetics reproduced herein, Figure 1. Those sigmoidal kinetic curves are well-fit by the two-step mechanism of nucleation and autocatalytic growth developed by one of us,[30] A → B with rate constant k_1, then A + B → 2B with rate constant k_2, where A = [RhCp*Cl$_2$]$_2$ and B = the catalytically active species. The kinetics are unequivocal in revealing that the starting complex A = [RhCp*Cl$_2$]$_2$ is not the catalyst but, instead, is a precatalyst en route to the catalytically active species, "B". In other words, those previously missing kinetics and net, overall reaction stoichiometry, A → B, demonstrate that B must form before catalysis ensues. The next question became—and still is—"what is B?"

A short summary of the evidence for "B" prior to the present study follows next, as that evidence, and the traps and pitfalls in interpreting it are important both in order to appreciate what follows and so that the broader community can understand the pitfalls, as well as fully capture the key insights, from this challenging case study. Central here en route to deducing the correct answer as to the true catalyst is a complete, balanced stoichiometry for the precatalyst-to-catalyst conversion reaction (i.e., for A (= [RhCp*Cl$_2$]$_2$) → B in the above kinetic formulation of the problem). That is, and in the end, the answer as to "what is B?" could be as simple—or as complex, vide infra—as determining
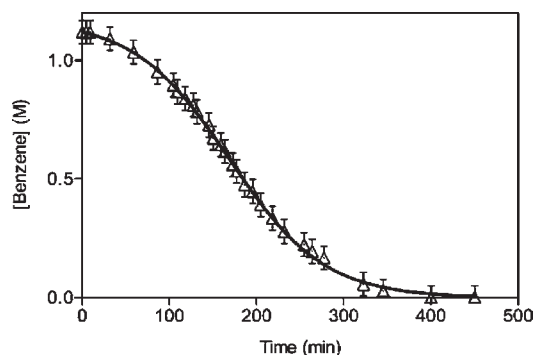
Figure 1. Data ($\triangle$) and curve fit (—) for a typical benzene hydrogenation reaction starting with $[RhCp^*Cl_2]_2$ in 2-propanol with added Et_3N at 100 °C and 50 atm initial H_2 pressure. The observed sigmoidal curve is well-fit ($R^2 = 0.999$) by the two-step mechanism A $\rightarrow$ B, A + B $\rightarrow$ 2B, with rate constants $k_1 = 7.1 \times 10^{-2}$ h^{-1} and $k_2 = 2.1 \times 10^2$ $M^{-1}h^{-1}$. This repeat experiment was performed as part of the present study to test the kinetic reproducibility of the system. The results reproduce our previously published data[27] of $k_1 = 1.9 \times 10^{-2}$ h^{-1} and $k_2 = 2.6 \times 10^2$ $M^{-1}h^{-1}$ within experimental error, given the $\sim10^{1.2}$ range historically seen in the k_1 nucleation rate constant.[31]

the product(s) under the precise reaction conditions, that is, *in operando*, vide infra.

The 2005 study reported that a black, Rh-containing precipitate is formed at the end of the reaction, a result verified herein by both CSU and Pacific Northwest National Laboratory (PNNL) groups, vide infra. Ex situ XPS analysis as part of the 2005 study identified the product as $Rh(0)$,[27] seemingly providing strong evidence for "$B = Rh(0)$"—albeit ex situ evidence. A control experiment filtrating the resultant solution using a 0.2 μm nylon syringe filter argued against bulk, low-surface area $Rh(0)_n$ as the catalytically active species, since any filterable precipitate did not provide a kinetically competent rate of benzene hydrogenation.[27] Complete poisoning of the catalyst was observed upon the addition of $\sim$300 equiv $Hg(0)$ per equiv of rhodium—again suggestive, but not definitive, evidence for of polymetallic, heterogeneous nanoparticle catalysis (i.e., given the problems and ambiguities in interpreting $Hg(0)$ poisoning experiments as discussed elsewhere[2] and as will be apparent from the $Hg(0)$ poisoning results herein). Ex situ TEM investigation in 2005 of the resultant catalyst solution dried on a TEM grid revealed the presence of 1.9 $\pm$ 0.5 nm, albeit poorly formed/somewhat "smeared" appearing, $Rh(0)_n$, nanoparticles. Significantly, TEM control experiments further revealed that just the $[RhCp^*Cl_2]_2$ precatalyst (diluted in 2-propanol, benzene, and triethylamine, then placed on a TEM grid) yielded similar, smeared appearing, 1.7 $\pm$ 0.3 nm $Rh(0)_n$ nanoparticles. Hence, the TEM evidence for $Rh(0)_n$ nanoparticles as a result of the catalytic reaction was, at best, rendered equivocal. In the end, the evidence that $B = Rh(0)$ came back to the black, ex situ XPS characterized $Rh(0)$ product. And, since there was no other precedented hypothesis at the time that could explain the available data, it seemed like a safe conclusion that the $[RhCp^*Cl_2]_2$ evolved at 100 °C and 50 atm H_2 pressure to $[Rh(0)_n\cdot(Cl^-Et_3NH^+)_m]$ nanoparticles as the most probable true catalyst,[27] a conclusion reinvestigated herein and shown to be in error.

In the mean time, studies at PNNL were focused on amine—borane dehydrocoupling prototype reactions starting with a $[Rh(1,5-COD)Cl]_2$ (COD: cyclooctadiene) precatalyst.[4] That work re-examined prior studies interpreted as $Rh(0)_n$ nanoparticle catalysis of amine—borane dehydrocoupling.[32] Significantly, in operando X-ray absorption fine structure (XAFS) spectroscopy revealed that >98% of the soluble Rh mass during the catalysis is present as amine—borane-stabilized, Rh_4 subnanometer clusters.[4,33] Importantly, principal component analysis (PCA) confirmed that no more than 2% of a third component could possibly be present in the *in operando* reaction cell constructed for the measurements. An upper limit of <1−2% was placed on the possible amount of soluble $Rh(0)_n$ present (in comparison to authentic $Rh(0)$ metal examined as a control and XAFS standard).

Next, in what are very important observations relevant to the present studies, a black precipitate formed in the later stages of the reaction (and which gives rise to a clear solution plus the black precipitate after 72 h) was shown by XAFS not to be the anticipated $Rh(0)_n$ nanoparticles. Instead, that black precipitate was proposed to be linked Rh_4 clusters on the basis of the XAFS data. In a second, significant observation a dehydrocoupling reaction done under O_2 led to the formation of a precipitate exhibiting the XAFS of—surprisingly—bulk $Rh(0)_n$, formed apparently via some sort of still ill-understood oxidation-induced, metal-reduction reaction. This result shows that ex situ analyses of black precipitates in air in at least the Rh/amine—borane system have considerable potential to yield very misleading results. In further studies directly relevant to the present work, four other Rh precursors were shown to evolve under the amine—borane dehydrocoupling reaction conditions (but not the benzene reduction conditions herein) to analogous ligand-stabilized Rh_4 clusters, including $[RhCp^*Cl_2]_2$, the precatalyst of the present benzene hydrogenation investigations.

The 2007 PNNL study concluded that the Rh_4 clusters are the leading true catalyst candidates for the amine—borane dehydrocoupling reaction.[4] Unfortunately, the needed rate law, poisoning, and other kinetic studies required to support or definitively refute the "Rh_4 subnanometer cluster catalysis hypothesis" in the amine—borane dehydrocoupling reaction have not yet been performed.[4] Hence, the identity of the true catalyst in the amine—borane dehydrocoupling reaction became, and remains, controversial. The authors of the first study using the $[Rh(1,5-COD)Cl]_2$ precatalyst for amine—borane dehydrocoupling still prefer their original conclusion, namely that the true catalyst is $Rh(0)_n$ nanoparticles.[34] Those authors note the lack of kinetic work in the second study[4] and point out that in air—where $Rh(0)_n$ has been shown to form in the PNNL study[4]—a drastically shortened induction period is observed. That case history reteaches the lesson from Halpern, namely that "catalysis is a wholly kinetic phenomenon",[10] again at least once favorable reaction thermodynamics are in place. Restated, one cannot possibly learn the identity of the true catalyst, for any catalytic reaction, without employing the necessary kinetic studies. As we will see herein, this includes the appropriate kinetic poisoning experiments in some cases, such as the present, and when polymetallic species are among the possible catalysts.

However, the PNNL work[4] proved central to—and indeed gave rise to—the present work by supplying the previously missing alternative hypothesis investigated herein: that ligated $Rh_{\sim4}$ clusters are actually the true catalysts for benzene hydrogenation beginning with $[RhCp^*Cl_2]_2$ in 2-propanol with added Et_3N at 100 °C and 50 atm H_2. Hence, herein the CSU and PNNL groups have joined forces to try to answer unequivocally the question of the true, kinetically dominant catalyst in the classic Maitlis benzene hydrogenation system, beginning with

$[RhCp*Cl_2]_2$ and 50 atm initial H_2 pressure at 100 °C. It is the required studies which are reported next.
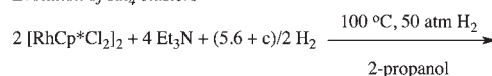
■ RESULTS AND DISCUSSION

Controls Repeating Key Experiments, Product Observations, and Construction of a Working Catalyst Evolution Stoichiometry. To start, controls repeating the hydrogenation of benzene, starting with $[RhCp*Cl_2]_2$ at 100 °C and 50 atm initial H_2 pressure, were performed according to the 2005 procedure.[27] Also repeated were Hg(0) poisoning and GC-MS investigation of the amount of hydrogenated Cp* released, initially as Cp*-H. These experiments were done to check the broad reproducibility of the catalyst evolution and resultant benzene hydrogenation system. Pleasingly, each of these repeat experiments yielded the same results as published previously[27] within experimental error. Specifically, (i) a sigmoidal benzene hydrogenation curve is again obtained (in seven repeat experiments throughout the course of these studies), kinetics that are nicely fit ($R^2 = 0.999$) to the two-step mechanism of autocatalytic catalyst evolution,[30] data shown back in Figure 1; (ii) the addition of ~300 equiv of Hg(0) per Rh, after one-third of a standard conditions benzene hydrogenation reaction is finished, kills the catalytic activity completely (Figure SI-1, Supporting Information) as previously observed;[27] and (iii) GC-MS investigation of the resultant solution reveals the release of free Cp*-H and its hydrogenation products, $Cp*-H_3$ and $Cp*-H_5$ at a level of ~42% of the initial Cp* present (Table SI-1, Supporting Information). The ~42% Cp* release results are identical within experimental error to those we previously reported, ~45%,[27] results which will also be fortified by a ca. 40% Cp* loss according to XAFS, vide infra. Interestingly, when one opens the Parr reactor after ~6 h in the drybox, (iv) one sees a dark-green solution suggestive of the presence of a tetrarhodium species,[29] such as "$Rh_4Cp*_{\sim2.4}Cl_bH_c$", where the $Cp*_{\sim2.4}$ value has been set from the Cp* loss value of ca. 40%. A black precipitate, plus the formation of a black film on the walls of the glass liner, is also seen in the Parr reactor opened in the drybox (that black precipitate previously believed to be Rh(0) from ex situ XPS[27] but which in operando XAFS will characterize as linked/agglomerated discrete, on average Rh_4 clusters, vide infra). Interestingly, (iv) fast atom bombardment-mass spectroscopy (FAB-MS) investigation of the rhodium product, right after the benzene hydrogenation is complete in ~6 h, reveals a molecular ion peak at $m/z = 956$ attributable to fully Cp*-ligated $[Rh_4Cp*_4H_4]^+$; that MS includes an excellent match to the calculated, theoretical isotope distribution pattern for a Rh_4 cluster, Figure SI-2, Supporting Information. Overall, a mixture of Rh_4Cp*_a species is implied, any mixture so long as the average "*a*" value is ca. 2.4, $Rh_4Cp*_{2.4}$ (i.e., and after ca. 6 h, when the benzene hydrogenation is complete, Figure 1). Combined together, the GC-MS and FAB-MS (and upcoming XAFS) results allow the suggested, average Rh evolution stoichiometry given in Scheme 2 to be written. Worth emphasizing here is that the "$Rh_4Cp*_{2.4}Cl_4H_c$" written is not intended to indicate a single Rh_4 species; any mixture of $Rh_4Cp*_aCl_bH_c$ that averages out to $a = 2.4$ and $b = 4$ will account for the observed data.

As a control and in expectation that longer reaction times would yield higher levels of Cp* loss from the $[RhCp*Cl_2]_2$ precatalyst, the level of Cp* loss after ~11 h reaction time in the Parr reactor was measured by GC-MS (i.e., and in comparison to the ~6 h "standard time" in Figure 1, vide supra, when all the benzene, but only ca. 16.3 atm of the initial 50 atm H_2, has been
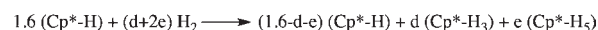
Scheme 2. Average Stoichiometry for the Evolution of the $[RhCp*Cl_2]_2$ Precatalyst into, on Average, $Rh_4Cp*_{\sim2.4}Cl_4H_c$ Clusters via GC-MS, FAB-MS, and XAFS (vide infra) Investigations

Evolution of Rh₄ clusters

$$2\ [RhCp*Cl_2]_2 + 4\ Et_3N + (5.6 + c)/2\ H_2 \xrightarrow[\text{2-propanol}]{100\ °C,\ 50\ atm\ H_2}$$

$$Rh_4Cp*_{2.4}Cl_4H_c + 4\ Et_3NH^+Cl^- + 1.6\ (Cp*-H)$$

Follow-up Cp-H Hydrogenation Reaction*

$$1.6\ (Cp*-H) + (d+2e)\ H_2 \longrightarrow (1.6-d-e)\ (Cp*-H) + d\ (Cp*-H_3) + e\ (Cp*-H_5)$$

consumed). As expected, additional Cp* was lost with the additional 5 h of reaction: ~73% Cp* loss after 11 h vs ~42% after 6 h. This experiment reveals that the average stoichiometry in Scheme 2 applies to the 6 h reaction time post which the benzene hydrogenation is complete.

However, the formulation of even the average, $Rh_4Cp*_{2.4}Cl_4H_c$, species present in solution after 6 h is still an important advance in addressing the true catalyst in this classic benzene hydrogenation catalysis system: it provides direct evidence for the hypothesis that "$Rh_4Cp*_{2.4}Cl_4H_c$" is the true catalyst (i.e., one or more of the species present that average to the stated, average molecular composition). The next order of business then became *in operando* XAFS studies to verify the proposed stoichiometry and to see if ~100% of the Rh mass could be accounted for by just Rh_4 species.

Investigation of the $[RhCp*Cl_2]_2$ Evolution Reaction via *In Operando* XAFS. *In operando* XAFS was employed to check and further reveal the average structural changes around rhodium atoms during the benzene hydrogenation and concomitant $[RhCp*Cl_2]_2$ evolution reaction. This enabled us to observe the evolution of what proved to be ligated Rh_4 clusters in a way that is impossible via ex situ analytical methods.[4,7]

In order to obtain the higher signal-to-noise ratio needed to search carefully for trace species (i.e., in particular any $Rh(0)_n$ nanoparticle formation, vide infra), four-fold more $[RhCp*Cl_2]_2$ was employed in the PNNL XAFS investigations compared to the CSU studies presented so far. Employing that four-fold higher concentration of $[RhCp*Cl_2]_2$ shortened the reaction time to a convenient, ca. ~1 h period (vs ~6 h under the CSU standard conditions, Figure 1). A control experiment was done showing that the XAFS results which follow are the same at the CSU conditions of one-fourth the concentration of $[RhCp*Cl_2]_2$ (Figure SI-3, Supporting Information).

To begin, a stirred batch reactor for *in operando* XAFS investigations was constructed from a stainless steel "tee" fittings (9/16 in., HIP, Erie, PA) plus custom PEEK (polyether ether ketone) windows that allow transmission of the X-ray beam, Figure 2. This continuously stirred, pressured reactor allowed the desired *in operando* XAFS measurements.

Figure 3 shows a time series of rhodium K-edge *in operando* X-ray absorption spectra of the benzene hydrogenation reaction accomplished with the cell shown in Figure 2. The primary feature of this raw data spectrum is the presence of three distinct isosbestic points.[35] Those isosbestic points provide strong evidence that the starting material is being converted into primarily a single new rhodium species as the reaction proceeds.[35] The *in operando* XAFS confirms the kinetics, and the two-step mechanism
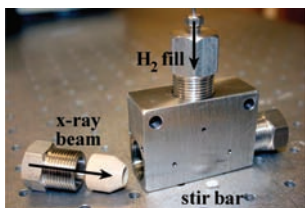
Figure 2. Continuously stirred reactor constructed and used for the *in operando* XAFS investigations herein of benzene hydrogenation starting with $[RhCp*Cl_2]_2$ at 100 °C and 50 atm initial H_2 pressure.
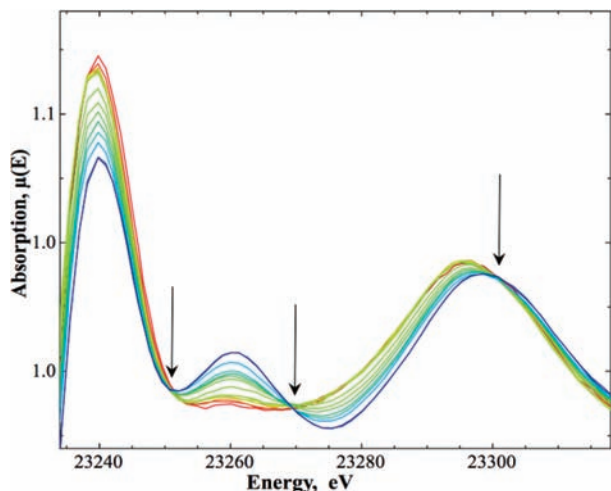

Figure 3. Series of time-dependent rhodium K-edge *in operando* XAFS spectra showing three distinct isosbestic points (indicated by the arrows) revealing that the precatalyst $[RhCp*Cl_2]_2$ is evolving to primarily a single new form of rhodium during the catalysis.

Figure 4. (a) Radial structure plot of the reaction progress showing an increase at around 2.7 Å attributed to Rh—Rh formation and a decrease at around 1.8 Å for Rh–Cp* and Rh—Cl interactions. (b) Coordination numbers for Rh, Cl, and Cp* about Rh as a function of the reaction time derived from fitting the *in operando* XAFS results to FEFF8 theoretical standards,[36] as detailed previously.[4] Note that although the starting material has a Rh—Cl CN of 3 initially, an XAFS experimental Rh—Cl CN of ~3.5 is observed at the start of the reaction, revealing an initial ~17% experimental error in the Rh—Cl CN, one consistent with an expected XAFS uncertainty of ±20% for the CN.

curve fits back in Figure 1: namely that $[RhCp*Cl_2]_2$ is a precursor to the dominant form of rhodium in solution once catalysis ensues post the induction period, A → B, necessary to begin to make that catalyst, "B".

Significantly, the new rhodium species, B, has a Rh—Rh bond length of ca. 2.7 Å, as given in the radial structure plot (RSP) with increasing Rh—Rh interaction, Figure 4a. For comparison, the starting material, $[RhCp*Cl_2]_2$, has a Rh—Rh distance of about 3.7 Å with no direct Rh—Rh bonding, Table 1. Figure 4a also shows the loss of the 1.8 Å feature, interpreted as the loss of Cp* and Cl ligands, a result consistent with the independent GC-MS results showing ca. 42% loss of Cp*. These features are summarized in Figure 4b which shows the time dependence of the rhodium coordination number (CN) for nearby rhodium, chloride, and Cp* ligands derived from fitting the experimental data to FEFF8 theoretical standards,[36] all done as detailed previously.[4] The average Rh—Rh CN increases quickly to ~3, that is, to on average Rh_4 clusters,[37] concomitant with Rh—Cl and Rh-Cp* CNs decreasing on average to ~1 and ~0.6, respectively. This is a central and key result: the hypothesis that Rh_4 clusters are the true catalyst is provided by the XAFS results.

As the reaction proceeds, the Rh-Cp* coordination number calculations from the XAFS data show a decreased CN around the new rhodium species, while the Rh_4 core is maintained, Figure 4b. However, since XAFS analysis is not very sensitive to the light, third-shell atoms around the Rh_4 core (e.g., C, O, Cl, etc.), one cannot obtain reliable information about the percentages of
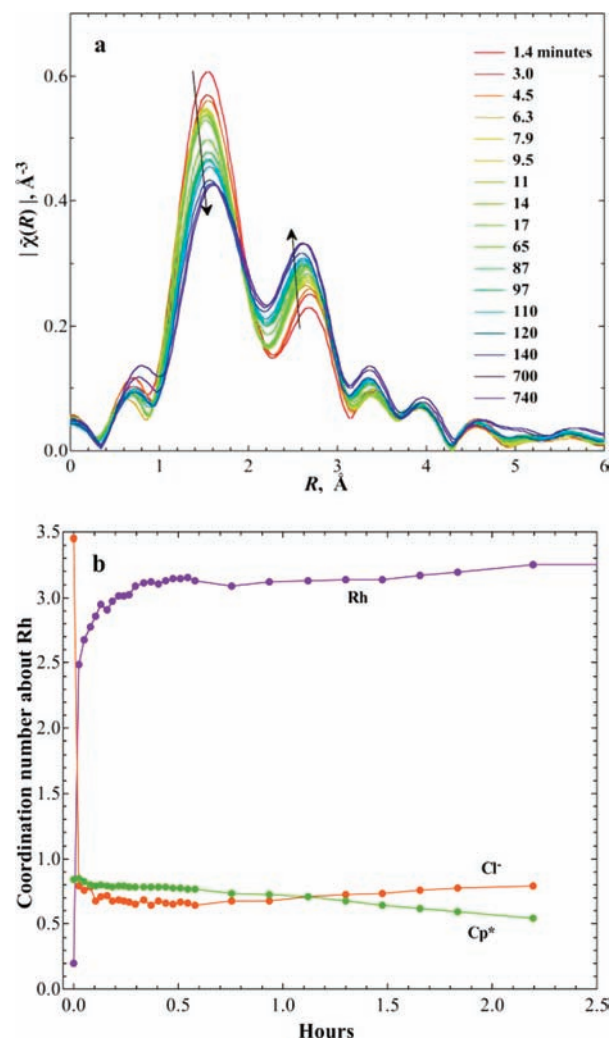
possible mixtures with the same Rh_4 core but different coordination numbers such as (but not limited to) Rh_4Cp*_4 or Rh_4Cp*_2. The only requirement is that the species present must average to a ca. 40% Cp* loss (i.e., or ca. 60% Cp* retention as found by XAFS, vide infra). The results in Figure 4 also reveal that the precatalyst transformation is largely accomplished within 0.5–1.0 h, under the four-fold higher $[RhCp*Cl_2]_2$ starting concentrations, so that the precatalyst evolution should be complete under ca. 4 × (0.5 to 1.0) h = ca. 2 to 4 h under the four-fold more dilute, CSU conditions (and assuming a first-order dependence on the concentration as will be shown to be the case, vide infra). Additional XAFS and other data reveal additional hydrogenated Cp* loss at longer times, however, vide supra.

When the benzene hydrogenation was complete (as judged by the cessation of H_2 uptake and ^1H NMR), XAFS parameters of

18893

dx.doi.org/10.1021/ja2073438 |*J. Am. Chem. Soc.* 2011, 133, 18889–18902

Table 1. Results of the EXAFS Analyses for [RhCp*Cl₂]₂ in Solid State and the Average Rh₄ Clusters Observed at the End of the Hydrogenation Reaction[a]

	EXAFS					XRD[38]
	scatterer	CN	R, Å	$\sigma^2 \times 10^3$, Å^2	$\mathscr{R}$[b]	R, Å
[RhCp*Cl₂]₂ in solid state (as boron nitride pellets)	Rh-Cp*	1	2.126 ± 0.006	3.0 ± 0.5	0.01	2.128
	Rh-Cp*CH₃	1	3.218 ± 0.017	5.1 ± 2.0		3.252
	Rh-Cl	2 + 1[c]	2.442 ± 0.015	5.0 ± 2.0		2.424
	Rh-Rh	1	3.725 ± 0.042	8.1 ± 2.9		3.719
Rh₄ clusters formed in solution after the catalysis	Rh-Cp*	0.6 ± 0.1	2.219 ± 0.012	5.2 ± 1.7	0.02	
	Rh-Cp*CH₃	0.6	3.282 ± 0.020	3.9 ± 2.1		
	Rh-Cl	1.3 ± 0.6	2.320 ± 0.029	12.8 ± 7.6		
	Rh-Rh	2.9 ± 0.4	2.714 ± 0.004	6.8 ± 0.6		

[a] In all cases the k^2 weighting was used for the fit. [b] Goodness of fit defined by a scaled sum of squares as described in FEFFIT.[36] [c] EXAFS is unable to resolve the two different Cl ligands of [RhCp*Cl₂]₂ (1 bridging +2 terminal per Rh) so they were modeled as an average.
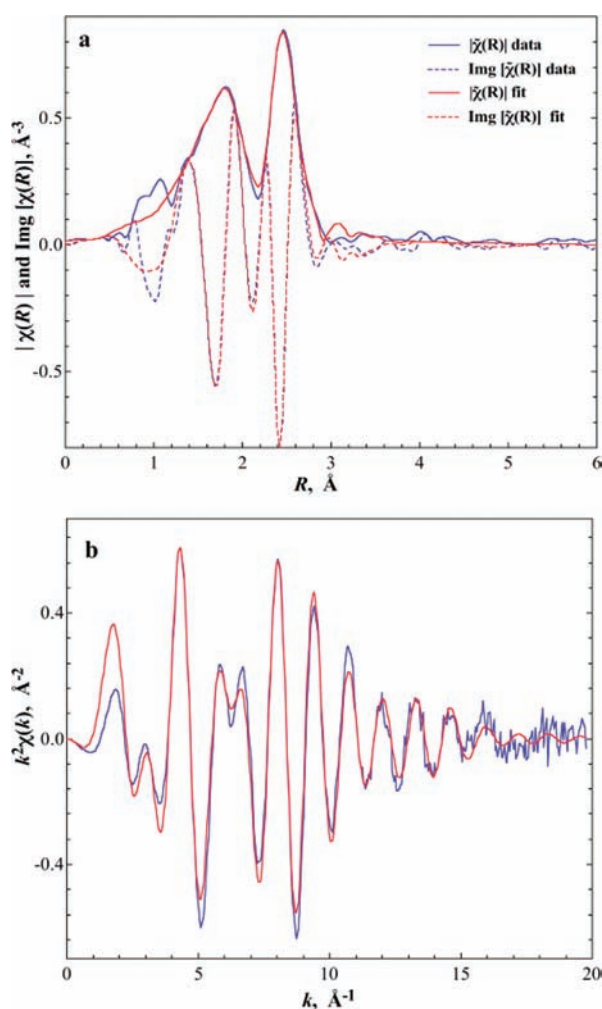

Figure 5. The k^2-weighted (a) $|\tilde{\chi}(R)|$ and $\text{Im}[\tilde{\chi}(R)]$ and (b) $\chi(k)$ plots for the Rh₄ clusters formed at the end of the complete benzene reduction. The experimental data, and the model fits[36] shown, reveal generally good agreement between the two.

the final solution were fit to FEFF8 theoretical standards.[36] Excellent fits to the experimental data were obtained, Figure 5. Table 1 provides the structural details of the Rh₄ clusters derived from these fits. Table 1 also includes the starting complex

[RhCp*Cl₂]₂ for a comparison of CNs and bond lengths and the control of comparing the XAFS results with the published crystal structure data of [RhCp*Cl₂]₂.[38] Noteworthy is that, in the new Rh species, there is no evidence, within the detection limits of XAFS, for any backscattering from either third or fourth rhodium shells. Restated, "no" (i.e., ≤2%) $Rh(0)_n$ nanoparticles could be detected by *in operando* XAFS.

The detailed analysis of XAFS data of the on average Rh₄ cluster product shows that all the CNs are different than those for the [RhCp*Cl₂]₂ starting material, Table 1. The most noticeable difference is the increase in the Rh−Rh CN from 1 to 2.9 ± 0.4 concomitant with a significant decrease in the Rh−Rh distance from the nonbonding value of 3.725 Å to a directly bonded Rh−Rh value of 2.714 Å. This change is similar to that found for the catalysis of dehydrocoupling of amine−borane complexes starting with [Rh(1,5-COD)Cl]₂ precatalyst and in which amine−borane stabilized Rh₄ clusters are formed.[4] The relatively low Debye−Waller factor (0.0068 Å²) and the high quality of the k^2-weighted fit, Figure 5, suggest that all four rhodium atoms are equivalent in this cluster. Consistently, all Rh−Rh bond lengths for the Rh₄ cluster are equal with 2.714 ± 0.004 Å, a value somewhat longer than the Rh−Rh distance of 2.68 Å in bulk metal[39] but similar to that found previously[4] for Rh₄ clusters of 2.734 ± 0.005 Å.[40]

Each rhodium atom has an average Cl CN of 1.3 ± 0.6 with a distance of 2.320 ± 0.029 Å. The Rh-Cp* contribution has a distance of 2.219 ± 0.012 Å with a CN of 0.6 ± 0.1. However, in the absence of a similar, literature structure with complete structural details that we could use as a model (i.e., no such structure was found from an extensive literature search), XAFS has limited ability to yield a more detailed picture for the ligand environment around Rh₄ clusters. However, the XAFS does reveal the presence of ligated Rh₄ clusters, their average Rh CNs, and that no additional Rh_x species are detectable.

Noteworthy here is that the XAFS and GC-MS Cp* evolution results agree rather well in terms of the average Cp* content of the resultant dominant form of rhodium present: the XAFS yielded a Rh-Cp* coordination number of 0.6 ± 0.1 (implying that the average Rh₄ cluster is ligated on average by 2.4 Cp* molecules), while the GC-MS reveals a ∼42% Cp* loss from the starting material, equivalent to a ∼58% (or 0.6 × 4 = 2.4) Cp* retention after 6 h of catalysis. In both cases a Rh₄Cp*₂.₄ formulation results as shown back in Scheme 2. With the 1:1 Rh:Cl ratio found on average by XAFS (i.e., Rh₄Cl₄), the resultant
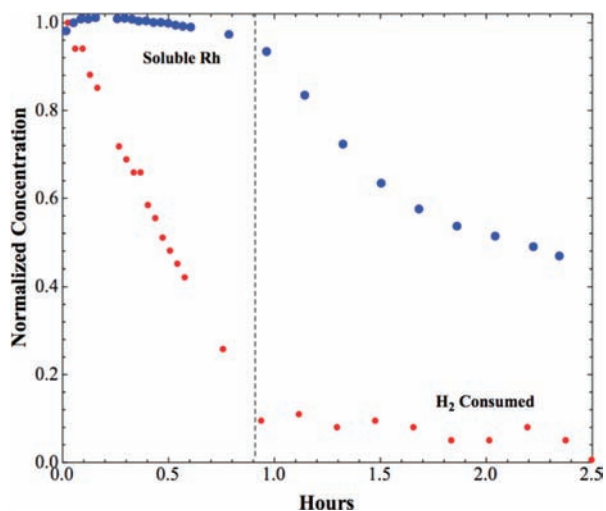
Figure 6. Normalized concentrations (via XAFS) of the ligated Rh_4 clusters and the H_2 pressure (measured simultaneously with the *in operando* XAFS) during and after benzene hydrogenation at 100 °C and 50 atm H_2 beginning with the $[RhCp*Cl_2]_2$ precatalyst. The final product analysis via ^{1}H NMR confirms that all the benzene initially present was converted into cyclohexane.

average Rh product becomes the "$Rh_4Cp*_{2.4}Cl_4H_c$" previously written in Scheme 2, with the caveat here that XAFS is unable to detect "H" ligands. Worth emphasizing again is that the formula "$Rh_4Cp*_{2.4}Cl_4H_c$" represents an average and is not intended to indicate a single Rh_4 species; any mixture of $Rh_4Cp*_aCl_bH_c$ that averages out to $a = 2.4$ and $b = 4$ is consistent with the XAFS and other data to this point. Nevertheless, the significant result is that the hypothesis that "$Rh_4Cp*_{2.4}Cl_4H_c$" is the true catalyst (i.e., one or more of the species present that average to these values) is now fortified by direct, *in operando* XAFS evidence.

XAFS Insights Into the Amount of Soluble Rh as a Function of Time and the Nature of the Black Precipitate. Since the XAFS edge height is proportional to the total amount of soluble rhodium in the X-ray beam (i.e., and for a constant beam path length as employed herein), edge height provides a fairly precise ($\pm2\%$) measure of the concentration of the soluble rhodium species, as detailed elsewhere.[4] The features in Figure 6 show that until complete conversion of the benzene (in ~1 h, at the four-fold higher concentrations used), the total amount of rhodium in solution via XAFS—identified as ligated Rh_4 clusters—stays relatively constant at $98 \pm 2\%$. After ~1 h, when 3 equiv of H_2 were consumed per benzene (via pressure measurements simultaneously with the *in operando* XAFS spectroscopy) and when ^{1}H NMR confirmed that all the benzene had been hydrogenated to cyclohexane, there is a marked reduction in the amount of soluble rhodium. The solubility of the Rh_4 cluster is reduced presumably because either "$Rh_4Cp*_{2.4}Cl_4H_c$" clusters that are no longer benzene ligated become insoluble in cyclohexane, perhaps they H-bridge (if Rh–H are present in the Rh_4 clusters), or the Rh_4 otherwise forms a black precipitate at the end of the reaction. This is the same black precipitate observed in the 2005 study[27] and now, independently, in both the PNNL and the CSU studies. Recall that it was this black precipitate, and the ex situ XPS evidence that suggested it was "Rh(0)", that ultimately mislead the prior study into believing that the black product of the reaction was the then expected black $Rh(0)_n$ nanoparticles.[27]

The experimental observations on the black precipitate are as follows: First, and again, (i) a black precipitate is observed in both the CSU and PNNL investigations, at the end of the reaction starting with $[RhCp*Cl_2]_2$ at 100 °C and 50 atm initial H_2 pressure, as well as a black film formation (on the PEEK windows of the reactor for PNNL investigation or on the glass liner of the Parr reactor for the CSU investigations); (ii) XAFS characterization of the black precipitate and black film at PNNL (in the fluorescence mode due to the low level of the black film) under O_2-free conditions showed the presence of Rh_4 clusters but no metallic rhodium nanoparticles within the $\pm2\%$ detection limits of XAFS; (iii) however, upon exposure to air, the black precipitate forms metallic rhodium by XAFS—a crucial observation that explains the previous observation of Rh(0) via ex situ XPS that included exposure to air.[27] Additional control experiments performed at CSU reveal that (iv) when the benzene hydrogenation is completed (~6 h) and the Parr reactor cooled, taken into the drybox to avoid any significant O_2 exposure, and then opened, a dark-green (i.e., Rh_4-like[29]) solution along with a black precipitate is observed (plus a black film formation on the walls of glass liner). Then, if 4 mL of fresh benzene are added to the reactor in the drybox, the reactor resealed, brought out of the drybox, and the Parr reactor reheated to 100 °C (without applying H_2 pressure) but then quickly opened in a hood with exposure to O_2/air, immediate visual inspection of the resultant solution reveals that the black precipitate had redissolved and a homogeneous, dark-green solution had formed. This simple experiment confirms the XAFS-derived absence of detectable, insoluble $Rh(0)_n$. This control further supports the XAFS conclusion that the black precipitate is not $Rh(0)_n$. However, if this dark-green solution is exposed to O_2/air in the hood, the solution becomes red-brown, and again a black precipitate is formed within 5 min (Rh(0) by ex situ XPS,[41] repeating the previous observation[27]). Overall, this control experiment fortifies the XAFS finding of Rh(0) formation from Rh_4 clusters via oxidatively induced metal reduction following exposure to O_2/air.

Overall, the XAFS studies are definitive in revealing that the black precipitate is not Rh(0) but, instead, is composed of soluble, apparently linked Rh_4 clusters—ones that, surprisingly, are reduced to Rh(0) under ex situ analyses involving exposure to O_2/air. The details of this presently somewhat mysterious "oxidatively induced metal reduction" reaction remain to be established, however, including its full reaction stoichiometry and the details of its underlying mechanism. Nevertheless, this unexpected observation of Rh(0) formation under O_2 exposure (and, presumably, concomitant ligand oxidation as the source of the reducing equivalents) is an important result. This unexpected result highlights the enormous potential of ex situ, non-*in operando* methods to mislead one completely regarding the true products of at least this particular system and its reactions.

Resultant Two Main Hypotheses for the True Catalyst. The sigmoidal kinetics, the A $\rightarrow$ B and A + B $\rightarrow$ 2B curve fit, the GC-MS, and now the XAFS results lead to the two main hypotheses for the true catalyst; hypotheses which will be the focus of the remaining parts of this paper, namely: (i) one or more forms of the ligated, on average "$Rh_4Cp*_{2.4}Cl_4H_c$" subnanometer clusters that comprise $98 \pm 2\%$ of the Rh mass are the true catalyst, or (ii) the possibly present, $\leq2\%$ of other form(s) of XAFS undetectable Rh are the true catalyst, for example, the previously suggested $[Rh(0)_n \cdot (Cl^-Et_3NH^+)_m]$ nanoparticles. Hence, kinetic experiments and the use of authentic $Rh(0)_n$ nanoparticles in control experiments as well as what turned out to be key quantitative
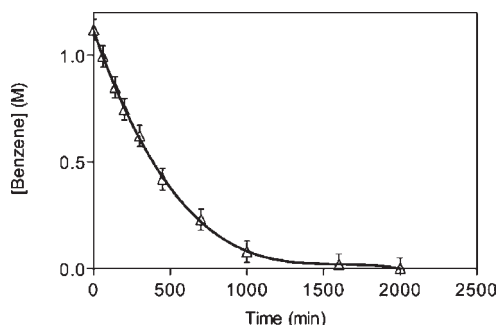
Figure 7. Benzene hydrogenation data (△) at 100 °C and 50 atm H_2 pressure employing the fully evolved catalyst initially started with 62.5 mg (0.101 mmol; 2.3 mM) [RhCp*Cl$_2$]$_2$. A polynomial fit to the data (—) with the equation $y = -2.7 \times 10^{-10} x^3 + 1.3 \times 10^{-6} x^2 - 0.0023x + 1.115$ to the data yielded an initial rate of $\{-d[\text{benzene}]/dt\}_{\text{in}} = 0.0023$ M/min. An important feature of this kinetic curve is the lack of an induction period.

kinetic poisoning experiments with 1,10-phenanthroline were performed next en route to ruling out one or more of the above hypotheses.

Kinetic Experiments Determining the Reaction Order of the ≥98% Rh$_4$ Species Present at the End of 6 h of Benzene Hydrogenation. By using predetermined amounts of initial [RhCp*Cl$_2$]$_2$ to change the concentration of the final Rh$_4$ solutions, the kinetics of the dependence on the rhodium species present at the end of the catalytic reaction was investigated. A simple first-order dependence would indicate if Rh$_4$, or any constant concentration, trace-level Rh species, is the true catalyst. Alternatively, some higher or fractional order dependence would indicate aggregated Rh$_4$ clusters or fragmented Rh$_4$ clusters are the true catalyst, respectively. Specifically, four separate standard conditions benzene hydrogenation starting with different amounts of [RhCp*Cl$_2$]$_2$ (62.5, 53.6, 44.3, or 27.2 mg) were performed. After the first benzene hydrogenation was completed, a subsequent benzene hydrogenation was started at the normal 100 °C and 50 atm initial H_2 pressure after the addition of 4 mL fresh benzene in the drybox, all as detailed in the Experimental Section. The resultant benzene hydrogenation curves were then fit to a polynomial equation in order to obtain the initial rates.[42] These kinetic curves are provided in Figure SI-4, Supporting Information, for the interested reader. One example curve, for an initial [RhCp*Cl$_2$]$_2$ amount of 62.5 mg (0.101 mmol or 2.3 mM under the reaction conditions) is provided in Figure 7. Significantly, no induction period is seen indicating that no further evolution of the XAFS observed ≥98% Rh$_4$ (or the possible ≤2% of other Rh species) is apparently necessary for catalysis.

The initial rate values obtained from the series of experiments allowed construction of Figure 8 showing a clean, first-order dependence on the [Rh]$_{\text{Total}}$ (i.e., ostensibly on the [Rh$_4$]^1), $R^2 = 0.998$. As a control, the same data set was tried in second- and half-order plots (i.e., the initial rate with respect to $\{[\text{Rh}]_{\text{Total}}\}^2$ and $\{[\text{Rh}]_{\text{Total}}\}^{1/2}$) but resulted in concave and convex curves, respectively, Figure SI-5a,b, Supporting Information), thereby confirming the better first-order fit.

The kinetic results are consistent with and supportive of the Rh$_4$ species present being the true catalyst. The results also rule out any higher order process or fragmentation where by the Rh$_4$ present would aggregate or fragment in either an irreversible step or a reversible, prior $K_{\text{eq}} \ll 1$ step. However, the kinetics alone do
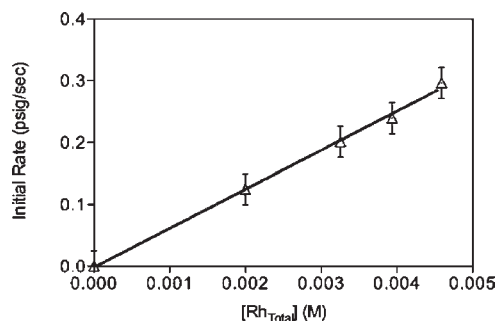

Figure 8. Plot revealing a clean first-order dependence ($R^2 = 0.998$) on the [Rh]$_{\text{Total}}$ formed at the end of an initial benzene hydrogenation reaction; conditions under which 98 ± 2% of the Rh is present as (average) Rh$_4$ subnanometer clusters.
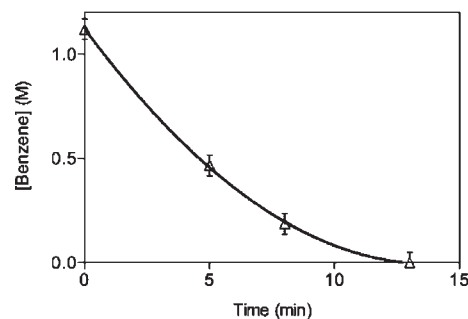

Figure 9. Benzene hydrogenation data (△) at 100 °C and 50 atm initial H_2 pressure employing polyethyleneglycol-dodecylether hydrosol stabilized Rh(0)$_n$ nanoparticles (231(±1) mg, 0.202 mmol Rh, the same amount of total Rh used in the standard conditions benzene hydrogenation beginning with [RhCp*Cl$_2$]$_2$). Also shown is a $y = 0.0058x^2 - 0.1624x + 1.1224$ polynomial fit (—) to the data.

not rule out other, trace Rh species, such as Rh(0)$_n$ nanoparticles, as the true catalyst, since the concentration of any such, reproducibly present trace species present would also change in a linear way in this experiment. Restated, the kinetics do not rule out trace, (i.e., ≪2%) but potentially high activity, Rh(0)$_n$ nanoparticles as the true catalyst. Hence this possibility was addressed next.

Benzene Hydrogenation Control Experiments at 100 °C and 50 atm Initial H_2 Pressure with Authentic Rh(0)$_n$ Nanoparticles as Model for Putative, XAFS Undetectable, ≤2% Rh(0)$_n$ Nanoparticles Possibly Present. Can Such Rh(0)$_n$ Nanoparticles Account for the Observed Catalytic Activity? Polyethyleneglycol-dodecylether hydrosol stabilized Rh(0)$_n$ nanoparticles that are ca. 2 nm and 9 wt % Rh were employed as model Rh(0)$_n$ nanoparticles. These Rh(0)$_n$ nanoparticles were picked since they should be "weakly ligated/labile ligand"[16] and thus good catalytic activity Rh(0)$_n$ nanoparticles as an example and model. For such ca. 2 nm Rh(0)$_n$ nanoparticles, ~40% of total rhodium atoms are on the surface according to a calculation using full shell, so-called "magic number" nanoparticles for this estimate.[43]

Employing the Rh(0)$_n$ nanoparticles in benzene hydrogenation under the normal standard conditions given in the Experimental Section was accomplished as follows: 231 ± 1 mg of polyethyleneglycol-dodecylether hydrosol stabilized Rh(0)$_n$ nanoparticles (0.202 mmol Rh, the same mmol as when [RhCp*Cl$_2$]$_2$ was used as a precatalyst) were added to a mixture of 36 mL of 2-propanol plus 4 mL of benzene.[44] Figure 9 shows the resultant

benzene hydrogenation curve. The authentic $Rh(0)_n$ nanoparticles both (i) showed no induction period—consistent with their being an active catalyst, and (ii) exhibited a superior, ca. 70-fold more active benzene hydrogenation catalyst activity on an equivalent, per rhodium basis in comparison to starting with the catalyst evolved from $[RhCp*Cl_2]_2$ after 6 h. The benzene reduction reaction was complete in <15 min and showed an initial rate of $\{-d[benzene]/dt\}_{in} = 0.1624$ M/min (vs a ~6 h total reaction time and initial rate of $\{-d[benzene]/dt\}_{in} = 0.0023$ M/min from Figure 7). TEM analysis of the final product revealed intact, albeit somewhat agglomerated, 2−3 nm $Rh(0)_n$ nanoparticles, Figure SI-6, Supporting Information.

The 70-fold greater reactivity allows the estimate that if even a mere $1/70 = ~1.4\%$ of the total Rh present initially in the $[RhCp*Cl_2]_2$ precatalyst is present as $Rh(0)_n$ nanoparticles, then those trace $Rh(0)_n$ nanoparticles could account for all the observed catalytic activity (all assuming that the polyethylene-glycol-dodecylether hydrosol stabilized $Rh(0)_n$ nanoparticles are a reasonable model of the activity of the nanoparticles postulated to be present as an alternative hypothesis for the true catalyst).[45] Significantly, ~1.4% is below the XAFS-undetectable upper limit of 2%. Just to check this result, one additional control was done of testing the activity of the model $Rh(0)_n$ nanoparticles at a 50-fold lower concentration (i.e., at a concentration equal to the 2% upper limit of other rhodium species that could be present). That experiment employed 4.04 μmol and 4.6 mg of polyethyleneglycol-dodecylether hydrosol stabilized $Rh(0)_n$ nanoparticles and resulted in an initial rate of $\{-d[benzene]/dt\}_{in} = 0.0032$ M/min, Figure SI-7, Supporting Information. This initial rate of 0.0032 M/min is still ca. 1.6-fold faster than the rate of the ≥98% Rh_4 solution, $\{-d[benzene]/dt\}_{in} = 0.0023$ M/min, Figure 7, vide supra. In short, trace, $Rh(0)_n$ nanoparticles, present at a level of ≤2% of the total Rh, are a kinetically competent catalyst.

The next question then became: are such $Rh(0)_n$ nanoparticles actually present and if so at what level, or is there another way to distinguish the two, still unrefuted hypotheses for the true catalyst: ≥98% Rh_4 subnanometer clusters or putative ≤2%, trace $Rh(0)_n$ nanoparticles? To attempt to refute one of these still remaining hypotheses, quantitative poisoning experiments were designed next and, fortunately, proved definitive in our opinion.

1,10-Phenanthroline Quantitative Kinetic Poisoning Experiments. The one and only quantitative poison candidate known at present to work both for benzene reduction catalysts and under ≥100 °C and ≥50 atm H_2 pressure is 1,10-phenanthroline.[46] Previously, 0.5 equiv of 1,10-phenanthroline (per metal) was shown to completely halt the catalytic activity at 110 °C and 60 atm H_2 pressure of what was in the end proposed to be a $Ru(0)_n$ nanoparticle benzene hydrogenation catalyst.[3]

Quantitative 1,10-phenanthroline poisoning experiments were performed as detailed in the Experimental Section. Specifically, the catalytic activities were tested as a function of the addition of 0.02, 0.5, 1.0, 2.0, 4.0, and 5.0 equivs (per total rhodium) of 1,10-phenanthroline (0.7, 18.2, 36.4, 72.8, 145.6, and 182 mg, respectively). The 1,10-phenanthroline was added to a fully evolved sample of catalyst post its ca. 6 h evolution. Significantly, when 0.02 or 0.5 equivs of 1,10-phenanthroline per Rh_{Total} were added, an initial rate of 0.0022 M/min was observed (Figure SI-8a,b, Supporting Information). That is, the catalytic activity did not change within experimental error after the addition of 0.02 or 0.5 equivs of poison per Rh_{Total} present (initial rate = 0.0023 M/min as was also seen in Figure 7). These results, while negative, argue against a $Rh(0)_n$ nanoparticle catalyst,

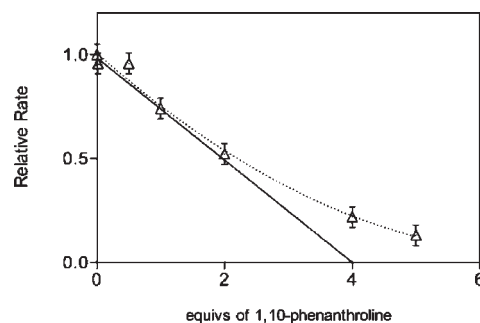**Figure 10.** Plot of relative initial rate vs equivs of 1,10-phenanthroline per total Rh for the benzene hydrogenation starting with 98 ± 2% ligated Rh_4 clusters according to XAFS. The linear, extrapolated portion of the data yields $x_{intercept} = 4.0 \pm 0.4$.
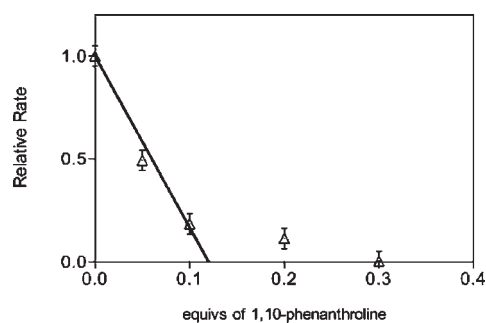
Figure 11. Plot of relative initial rate vs equivs of 1,10-phenanthroline per total Rh for benzene hydrogenation starting with polyethyleneglycol-dodecylether hydrosol stabilized $Rh(0)_n$ nanoparticles. The linear, extrapolated portion of the data yields $x_{intercept} = 0.12 \pm 0.02$.

especially when the next set of experiments with higher 1−5 equivalents of poison are considered.

Significantly, the addition of 1, 2, 4, and 5 equivs of 1,10-phenanthroline per Rh_{Total} did slow the initial catalytic activity, from $\{-d[benzene]/dt\}_{in} = 0.0023$ M/min to $\{-d[benzene]/dt\}_{in} = 0.0017, 0.0012, 0.0005$, and 0.0003 M/min, respectively, Figure SI-8c−f, Supporting Information. Figure 10 reveals that ~4.0 equiv of 1,10-phenanthroline per total Rh poisons most, ca. 75%, of the catalyst's activity.[17] As is customary for such quantitative poisoning plots,[17,47] an $x_{intercept}$ was calculated from a linear regression analysis of the linear portion of the relative rate vs equivs of 1,10-phenanthroline per Rh_{Total}, Figure 10. That plot yielded an $x_{intercept} = 4.0 \pm 0.4$, implying that the amount of poison required to totally poison the active catalyst is ≥4.0 equivs of 1,10-phenanthroline per Rh_{Total}. These poisoning findings are consistent with and strongly supportive of the *in operando* XAFS detected Rh_4 clusters being the true catalyst, especially in light of the control experiments of poisoning the authentic $Rh(0)_n$ nanoparticles discussed next where the $x_{intercept} = 0.12 \pm 0.02$.

Next, polyethyleneglycol-dodecylether hydrosol stabilized $Rh(0)_n$ nanoparticles were examined in 1,10-phenanthroline poisoning control experiments, as detailed in the Experimental Section, using 0.05, 0.1, 0.2, and 0.3 equivs of 1,10-phenanthroline per total rhodium, Figure SI-9a−d, Supporting Information. As a plot of the relative rates vs equivs of 1,10-phenanthroline per Rh_{Total} graph makes clear (Figure 11), these authentic $Rh(0)_n$ nanoparticles are poisoned by ≪1.0 equiv of poison. The $x_{intercept} = 0.12 \pm 0.02$, a value far smaller and unequivocally distinguishable
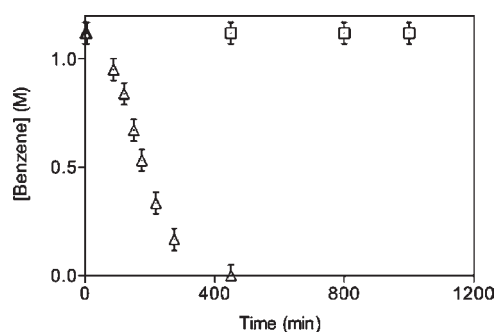
Figure 12. The addition of ~300 equiv of Hg(0) per total Rh plus good stirring poisoned completely (□, data) the catalytic activity of a solution of previously active (△, data) 98 ± 2% Rh$_4$ clusters. The results indicate that Rh$_4$ benzene hydrogenation catalysis is fully poisoned by excess Hg(0).

from the $x_{intercept}$ = 4.0 ± 0.4 for the solution composed of ≥98% of XAFS-detected, subnanometer Rh$_4$ clusters.

The combined poisoning studies make a very strong case that the on average Rh$_4$ subnanometer clusters are the most active benzene hydrogenation catalyst present—that is, that one or more of the Rh$_4$Cp*$_{2.4}$Cl$_4$H$_c$ species present is the true benzene hydrogenation catalyst in the present system and under the 100 °C and 50 atm H$_2$ initial pressure conditions in 2-propanol and with added Et$_3$N. The other insight remains, however, that had even 1.4% of the soluble Rh been in the form or Rh(0)$_n$ nanoparticles, then those nanoparticles would have been the most active catalyst (and if those nanoparticles had the activity of the model polyethyleneglycol-dodecylether hydrosol stabilized Rh(0)$_n$ nanoparticles).

Additional Insights From the 1,10-Phenanthroline Poisoning Studies. Even for the present data one can make a couple of additional, interesting interpretations: First, the Rh(0)$_n$ nanoparticles probably bind the 1,10-phenanthroline more tightly (just looking at the shapes of the two poisoning plots, the curve for Rh$_4$ being more convex and thus suggesting a weaker binding constant), a point that argues against the one alternative interpretations of the present poisoning data that we can see which would have required a much higher binding constant of the poison by the Rh$_4$ clusters.[48] Second, if one takes the 0.12 $x_{intercept}$ of the Rh(0)$_n$ poisoing plot and divides by the 0.4 fraction of Rh on the surface, one calculates that 0.12/0.4 or 0.3 equivs of 1,10-phenanthroline per surface Rh are required to poison the Rh(0)$_n$ nanoparticles. Hence, a rather large fraction, ca. 30%, of the surface Rh of these specific polyethyleneglycol-dodecylether hydrosol stabilized Rh(0)$_n$ nanoparticles are active (or twice this, ca. 60%, if each 1,10-phenanthroline binds in a bidentate fashion, poisoning 2 sites). Additional quantitative model and mechanistic studies of the 1,10-phenanthroline poisoning studies are in progress, as they have the potential to strengthen further[48] the results presented herein and to yield more precise values of the numbers of active sites for both the Rh$_4$ and Rh(0)$_n$ catalysts.

One Additional Hg(0) Poisoning Experiment with the Now Identified, Subnanometer Rh$_4$ Cluster-Based Catalyst. Since it has previously often, but incorrectly,[2] been believed that a Hg(0) poisoning experiment can definitively distinguish homogeneous vs heterogeneous catalysis, a Hg(0) poisoning experiment was repeated on a sample of catalyst post its ~6 h evolution and where the average form of the Rh catalyst is now known to be 98 ± 2% Rh$_4$Cp*$_{2.4}$Cl$_4$H$_c$. Specifically, and as detailed in the

Experimental Section, the addition of ~300 equiv of Hg(0) (per rhodium) and fresh benzene (4 mL) to a previously fully active catalyst halted the catalyst activity completely, Figure 12. This experiment reveals for the first time that Hg(0) poisoning cannot distinguish M$_4$ from M(0)$_n$ catalysis, at least when M = Rh and for the present benzene hydrogenation system. This finding supports and further fortifies the conclusion that the Hg(0) poisoning test "is not definitive and is not universally applicable."[2] Hence, the Hg(0) test should be used and interpreted with considerable caution.

■ CONCLUSIONS

(i) The bulk of the evidence—and particularly the combination of *in operando* XAFS, kinetic and quantitative kinetic poisoning experiments—reveals that the true benzene hydrogenation catalyst, beginning with [RhCp*Cl$_2$]$_2$ at 100 °C and 50 atm initial H$_2$ pressure in 2-propanol and with added Et$_3$N, is in all probability one or more of the Rh$_4$ subnanometer clusters of average formula Rh$_4$Cp*$_{2.4}$Cl$_4$H$_c$.

(ii) The present studies, the history of this classic system, and the historical "is it single-metal homogeneous or polymetallic, nanoparticle heterogeneous catalysis?" question reveals that it is neither. Instead, appropriately ligand-stabilized subnanometer M$_4$ clusters can be the dominant catalyst in favorable situations and cases.

(iii) The results and the history of this challenging "who is the true catalyst?" case study reveal that one must use *in operando* spectroscopic methods, along with the appropriate kinetic and kinetic poisoning studies, to identify the true catalyst in at least this example. In one limiting view, this is nothing more nor less than what J. Halpern showed 30 years ago, albeit there for discrete, single-metal organometallic systems.[10] Catalysis is a kinetic phenomenon.[10]

(iv) Ex situ TEM investigations, ex situ XPS studies in air, and Hg(0) poisoning studies have each been shown to be ambiguous, if not highly misleading, when one is attempting to determine the true catalyst, at least in the present Rh catalysis system.

(v) Identifying the form of the bulk of the evolved precatalyst mass, even by the powerful *in operando* XAFS studies herein that identify >98% of the starting Rh present as Rh$_4$ clusters, is insufficient to identify the true catalyst. That is, *in operando* spectroscopic studies are necessary, but insufficient, for identifying the true catalyst. Kinetic investigations are a must. If even ~1.4% of the total Rh present had formed Rh(0)$_n$ nanoparticles with activity as good or higher than that exhibited by the polyethyleneglycol-dodecylether hydrosol stabilized model Rh(0)$_n$ nanoparticles, then those nanoparticles would have been the active catalyst.

(vi) And, finally, quantitative kinetic poisoning experiments are hereby added to the arsenal of the most important, if not necessary, experiments for distinguishing single metal from M$_4$ from M(0)$_n$ polymetallic catalysts—those kinetic poisoning studies being intrinsically "*in operando*". It will be of interest to see if such poisoning studies can now resolve the controversy over the active catalyst—Rh$_4$ subnanometer clusters vs Rh(0)$_n$ nanoparticles—in the amine borane dehydrocoupling area. In addition, some of our (i.e., R.G.F. and co-workers') interests are focused on a more detailed analysis of nanoparticle kinetic poisoning studies due to the broad application and potential importance to nanoparticle catalysis that such studies promise to have.

■ EXPERIMENTAL SECTION

In what follows, all details refer to experiments done at CSU except for the *in operando* XAFS, for which separate experimental details are reported.

Materials. Benzene (Aldrich, 99.8%, anhydrous, packaged under N_2), 2-propanol (Aldrich, 99.5%, anhydrous, packaged under N_2), and 1,10-phenanthroline (Aldrich, 99%) were transferred into the drybox and used as received. Elemental Hg(0) (Aldrich, 99.9995%) was brought into the drybox just before it was needed and then removed after that, since Hg(0) will poison the oxygen-scavenging Cu catalyst of the drybox. Triethylamine (Aldrich, 99.5%, packaged under N_2) was stored in a refrigerator and used as received. Hydrogen gas (General Air, 99.5%) was used as received. Deuterated NMR solvents were purchased from Cambridge Isotope Laboratories, Inc. $[RhCp*Cl_2]_2$ (99%) and Rh colloid (polyethyleneglycol-dodecyl ether hydrosol) ($\sim$9 wt % Rh, $\sim$2 nm Rh(0)$_n$ nanoparticles) were purchased from Strem Chemicals, stored in the drybox, and used as received.

For the In Operando XAFS. Benzene (Aldrich) was fractionally distilled twice from sodium, 2-propanol (Aldrich) was distilled from CaH_2, and triethylamine (Aldrich) was distilled from KOH. Reagent alcohol (Aldrich) and $[RhCp*Cl_2]_2$ (Strem Chemicals) were used as received.

General Procedures for Benzene Hydrogenation. All preparations and manipulations were performed under oxygen- and moisture-free conditions in a Vacuum Atmosphere N_2 drybox (<2 ppm of O_2 as continuously monitored by a Vacuum Atmosphere O_2 monitor), unless indicated otherwise. All benzene hydrogenations were performed in a Parr pressure reactor (model 4561) made of Monel 400 alloy. The reactor is equipped with a pressure gauge marked at intervals of 20 psig ($\sim$1.36 atm) and an automatic temperature controller ($\pm$3 °C). Additionally, the inside of the reactor contains a stainless steel (i.e., non-Monel) impeller, thermocouple, cooling loop, and dip tube; all these components are in contact with the reaction solution. A glass liner was used to avoid contacting the reaction solution with the rest of the reactor. The glass liner was dried overnight in a 160 °C drying oven before being transferred into the drybox. Pressurizing the reactor took about 1 min, and t = 0 was set once the reactor was fully pressurized. Pressure gauge readings vs time data were then collected and recorded.

Standard Conditions Benzene Hydrogenation with $[RhCp*Cl_2]_2$. In the drybox, 62.5 ($\pm$1) mg (0.101 mmol) of $[RhCp*Cl_2]_2$ was quantitatively transferred into an oven-dried glass liner with 36 mL of 2-propanol and 4.0 mL (44.8 mmol) of benzene, yielding a clear, orange solution with some undissolved $[RhCp*Cl_2]_2$ to start. Next, 0.41 mL (2.94 mmol) of Et$_3$N was added with a gas tight syringe, and the glass liner was sealed in the reactor. The reactor was removed from the drybox, stirring was started at 600 rpm, equilibrated at 100 °C, and pressurized to 740 psig (50 atm) with H_2. Under these conditions, complete conversion of benzene to cyclohexane corresponds to a pressure loss of about 240 psig, ($\sim$16.3 atm), see the calculation below. At the end of each hydrogenation reaction, and as a control to avoid attributing possible reactor leaks to hydrogenation activity, the percent conversion of benzene into cyclohexane was verified directly by ^{1}H NMR analysis (via Varian INOVA-300 instrument at 300 MHz for ^{1}H). In those control experiments, the NMR sample was prepared by adding a drop of the final reaction solution into 1 mL CD_2Cl_2, and the resultant solution examined by ^{1}H NMR for the singlet at 1.4 ppm for cyclohexane and also the absence of benzene singlet peak at 7.2 ppm. Seven repeats of this standard conditions experiments were performed, all of which showed hydrogen-uptake curves analogous to that given in Figure 1 within experimental error along with complete conversion of benzene into cyclohexane.

The pressure data were converted to benzene concentration data by a simple proportional relationship:[27] [benzene] = [benzene]$_{initial}$ ×

(pressure − pressure$_{final}$)/(pressure$_{initial}$ − pressure$_{final}$). This treatment assumes that the pressure$_{final}$ corresponds to complete conversion of benzene to cyclohexane, as verified experimentally by ^{1}H NMR. The error bars shown for the benzene concentration assume an error of $\pm$10 psig ($\sim$0.68 atm) in the pressure gauge reading. A variability of $\pm$3 °C in the temperature control is also present with our Parr high-pressure apparatus.

Cleaning the Reactor between Benzene Hydrogenation Reactions and the Control of Testing the Residual Hydrogenation Activity of the Reactor Itself. The possible non-negligible hydrogenation activity of the reactor components was prevented by careful cleaning as described below, followed by checking a blank solution (i.e., 36 mL of 2-propanol, 4.0 mL of benzene, and 0.41 mL of Et$_3$N with no added $[RhCp*Cl_2]_2$) for residual activity prior to each catalytic run. Then, after a catalytic reaction, the Parr reactor parts in contact with the reaction solution were carefully cleaned by scrubbing with a steel wool pad and then rinsed with water, nitric acid, and distilled water. This cleaning procedure, and resultant control checking for residual activity, gave no measurable H_2 loss (0 psig) over 5 h in every case.

Hg(0) Poisoning Experiments. Two separate Hg(0) poisoning experiments were performed. For the first one, a Standard Conditions Benzene Hydrogenation with $[RhCp*Cl_2]_2$ was started. Pressure vs time data were collected until the pressure had decreased to 660 psig ($\sim$44.6 atm), that is, until ca. one-third completion. Then the reactor was vented, cooled to room temperature, taken into the drybox, and opened. Next, 6.05 g Hg(0) ($\sim$300 equivs per Rh) were added to the reaction solution. The reactor was then resealed, brought out of the drybox, equilibrated at 100 °C, and repressurized to the prior 660 psig ($\sim$44.6 atm) with H_2. At this point the collection of pressure vs time data was resumed.

A separate standard conditions benzene hydrogenation with $[RhCp*Cl_2]_2$ was started for the second Hg(0) poisoning experiment. When the reaction was completed—as judged by the cessation of H_2 uptake and by the ^{1}H NMR of the product—the reactor was vented, cooled to room temperature, taken into the drybox, and opened. Next, 6.05 g Hg(0) ($\sim$300 equivs per Rh) and fresh benzene (4 mL) were added to the reaction solution. The reactor was then resealed, brought out of the drybox, equilibrated at 100 °C, and repressurized to the 740 psig (50 atm) with H_2. At this point the collection of pressure vs time data was started.

A control experiment (without the addition of Hg(0)) was performed to see if the procedure of releasing the remained H_2 pressure, cooling, opening the Parr reactor in the drybox, then resealing it, rewarming it, and reapplying the H_2 pressure caused any loss in catalytic activity. No change in the catalytic activity was observed within the experimental error. Hence, any changes in the catalytic activity must be due to the addition of Hg(0) (or 1,10-phenanthroline, vide infra) and not the physical procedure necessary to open up the Parr reactor, add Hg(0) (or add 1,10-phenanthroline, vide infra), and restart the reaction by repressurization with H_2 at 100 °C.

GC-MS Experiment Showing Cp* Ligand Loss from $[RhCp*Cl_2]_2$ via Observation of the Resultant Cp*-H and Its Hydrogenation Products. The details of this investigation are provided in the Supporting Information. The key result is that $\sim$42% of released, partially hydrogenated Cp* products are observed, within experimental error of the $\sim$45% detected previously.[27]

Additionally, the same GC-MS procedure was employed when the reaction was allowed to proceed for $\sim$11 h of prolonged reaction time (vs the $\sim$6 h in Figure 1, vide supra). Quantification of the resultant by GC-MS analysis revealed additional Cp* loss as the reaction proceeds for an additional 5 h, $\sim$73% Cp* loss after 11 h (vs $\sim$42% after 6 h), Table SI-1, Supporting Information.

Kinetic Investigation of the Rhodium Solution and Species Formed at the End of the Benzene Hydrogenation Reaction.

A Standard Conditions Benzene Hydrogenation with $[RhCp*Cl_2]_2$ was repeated four times but starting with different initial amounts of $[RhCp*Cl_2]_2$ of 62.5, 53.5, 44.3, and 27.2 mg in the 4 separate experiments. In these four independent experiments, the following procedure was used at the completion of the benzene hydrogenation (as judged by the cessation of H_2 uptake and by ^{1}H NMR of the product): the remaining H_2 pressure was released, the reactor was cooled, taken into the drybox, and opened. Then, 4.0 mL (44.8 mmol) of fresh benzene was added. The reactor was resealed and removed from the drybox, stirring was started at 600 rpm, equilibration to 100 °C accomplished, and then pressurized to 740 psig (50 atm) with H_2. At this point the collection of pressure vs time data was started.

The method of initial rates was used to analyze the kinetic data (see below for details). The hydrogenation curves for each trial, along with the polynomial equation and fit used to get the initial rates, are provided in Figure SI-4, Supporting Information.

Kinetic Data Treatment. *Initial Rate Method.* Initial rates were calculated from benzene concentration vs time or hydrogen pressure vs time data employing the initial rate method described elsewhere.[42] Briefly, the obtained data were fit to a second- or a third-degree polynomial equation using Microsoft Excel 2008; the polynomial that fits best, as judged by the highest R^2 value, was used. Taking the derivative of the polynomial equation with respect to time and evaluating it at $t = 0$ yields the initial rate (the coefficient of the second, initially t^1 term of the polynomial). For all initial rate calculations, the data, fit, and polynomial equation are provided in the Supporting Information. For all the initial rate determinations, the first ~25% of the data was also fit to a straight line as a check of the polynomial-determined initial rate; similar initial rates resulted in all cases. However, the initial rates obtained from the more rigorous procedure of the second- (or third-) order polynomial fits are what is reported in the Supporting Information.

Benzene Hydrogenation Starting with Polyethyleneglycol-Dodecylether Hydrosol Stabilized Rh(0)$_n$ Nanoparticles and Product Analysis via TEM. To start, 231 ($\pm$1) mg (0.202 mmol total Rh, the same amount as in the case of Standard Conditions Benzene Hydrogenation with $[RhCp*Cl_2]_2$) of polyethyleneglycol-dodecylether hydrosol stabilized Rh nanoparticles, ca. 2 nm, ~9 wt % Rh, was transferred quantitatively into an oven-dried glass linear with 36 mL of 2-propanol and 4.0 mL (44.8 mmol) of benzene,[44] followed by sealing of the reactor. The reactor was removed from the drybox, and stirring was started at 600 rpm, equilibrated at 100 °C, and pressurized to 740 psig (50 atm) with H_2. The collection of pressure vs time data was then started.

A sample for NMR was prepared by adding a drop of the resultant solution into 1 mL CD_2Cl_2 in the drybox. The complete conversion of benzene into cyclohexane was verified directly by ^{1}H NMR analysis by observing a singlet at 1.4 ppm for cyclohexane while also looking for the absence of singlet peak at 7.2 ppm for benzene.

A TEM sample was prepared in the drybox from the same, resultant solution. A 300 mesh Formvar-coated SiO_2 TEM grid was dipped into the sample solution for 5 s and allowed to dry. The grid was then placed in a 2 dram vial, and the TEM investigation was performed with JEOL 1400 instrument with 100 kV accelerating voltage. The TEM images of the resultant show the presence of somewhat agglomerated, 2−3 nm sized Rh(0)$_n$ nanoparticles (Figure SI-6, Supporting Information).

The above procedure was repeated for 50-fold lower concentration of Rh(0)$_n$ nanoparticles, corresponding to the upper limit of 2% of other possible rhodium species when starting with $[RhCp*Cl_2]_2$ under standard conditions. For this purpose, only the initial amount of polyethyleneglycol-dodecylether hydrosol stabilized Rh nanoparticles was changed to 4.6 mg (4.04 μmol) in a separate experiment (Figure SI-7, Supporting Information).

1,10-Phenanthroline Quantitative Poisoning Experiments for the Standard Conditions Benzene Hydrogenation with $[RhCp*Cl_2]_2$. For each quantitative poisoning experiments with 1,10-phenanthroline, a separate Standard Conditions Benzene Hydrogenation with $[RhCp*Cl_2]_2$ was started. When the reaction was completed—its completion being judged by the cessation of H_2 uptake and by ^{1}H NMR of the cyclohexane product—the reactor was vented, cooled to room temperature, taken into the drybox, and opened. Note that, from the XAFS results, 98 $\pm$ 2% of the total Rh in solution at this time is ligated Rh_4 clusters with $\leq$2% undetectable soluble Rh species. Next, 4 mL of fresh benzene plus a quantitative, predetermined amount of 1,10-phenanthroline were added to the solution; 0.02, 0.5, 1, 2, 4, and 5 equivs per total Rh (i.e., 0.7, 18.2, 36.4, 72.8, 145.6, and 182 mg, respectively). The reactor was then resealed, brought out of the drybox, equilibrated at 100 °C, and repressurized to 740 psig (50 atm) with H_2. At this point the collection of pressure vs time data was started.

The resultant poisoning data were then fit to a polynomial, as detailed previously, to obtain the initial rate for each experiment. The kinetic curves along with the polynomial fits are provided in Figure SI-8, Supporting Information.

1,10-Phenanthroline Quantitative Poisoning Experiments for Polyethyleneglycol-Dodecylether Hydrosol Stabilized Rh(0)$_n$ Nanoparticles. For each quantitative poisoning experiment using these authentic, commercial Rh(0)$_n$ nanoparticles plus 1,10-phenanthroline, a separate Benzene Hydrogenation Reaction Starting with Polyethyleneglycol-Dodecylether Hydrosol Stabilized Rh Nanoparticles was performed, as detailed above, except with one change: a quantitative, predetermined amount of 1,10-phenanthroline was added to the initial solution. For this purpose, 0.05, 0.1, 0.2, and 0.3 equiv 1,10-phenanthroline (i.e., 1.8, 3.6, 7.2, and 10.8 mg, respectively) per total Rh was added for each separate poisoning experiment. The resultant hydrogenation curves for each trial were fit to a polynomial, and the initial rate was calculated as detailed previously with the results shown in Figure SI-9, Supporting Information,

Standard Conditions Benzene Hydrogenation with $[RhCp*Cl_2]_2$. *In Operando XAFS Investigation Details.* The same experimental procedure, data analysis, and fit methods were followed as detailed previously.[4] The rhodium K-edge (23 222 eV) XAFS spectra were collected in transmission mode on the bending magnet beamline (PNC-CAT, Sector 20) at the Advanced Photon Source, Argonne National Laboratory. The bending magnet beamline was chosen over the much higher flux insertion-device line to minimize the potential for beam damage to the rhodium complexes. No evidence of beam-created photoelectron or other damage was observed during exposure of the rhodium complexes to the X-rays. Details of the XAFS beamline methods are given elsewhere.[4] Portions of the Athena and Artemis programs were used for the analysis of XAFS data with theoretical standards calculated using FEFF8.[36] The XAFS $\chi(k)$ data were weighted by k^2 and windowed between $2.0 < k < 19.0$ Å^{-1} using a Hanning window with $dk = 1.0$ Å^{-1}. The fits were to both the real and imaginary parts of $\tilde{\chi}(R)$ in the region of $1.0 < R < 4.0$ Å. Five rhodium-containing standard compounds were previously used[4] to establish the value of the core hole factor, $S_0^2 = 0.89$. S_0^2 has an associated uncertainty of about 15% that results in an approximate 15% uncertainty in the reported coordination number. Strategies for generating appropriate theoretical standards have been previously discussed.[4]

Catalysis reactions for the *in operando* XAFS were conducted in a stirred reactor constructed from a stainless steel "tee" fittings (9/16 in., HIP, Erie, PA) that was fit with custom PEEK (polyether ether ketone, PEEK dupont) windows to allow for transmission of the X-ray beam (Figure 2). The concentration of the $[RhCp*Cl_2]_2$ complex used for XAFS measurements was, by design for better signal-to-noise (S/N), 4-fold higher than that used for the standard conditions experiments at CSU. The increased S/N ratio of the resultant XAFS data allowed differentiation of the noise from any possible, low concentration, Rh(0)$_n$ nanoparticles. A control showed that reducing the concentration

4-fold to the CSU standard conditions yielded the identical XAFS spectrum but with poorer S/N ratio (Figure SI-3, Supporting Information), results that provide confidence in connecting the CSU and 4-fold higher concentration PNNL data.

In all XAFS experiments, the reactor was initially loaded with the reaction solution in a glovebox containing 4% H_2 in helium, sealed, and removed from the box. Just prior to reaction, the helium was replaced by three pressurizations with H_2 to 20 bar. The cell was placed in the XAFS beam, heated to the set point (i.e., 100 °C) using electrical-resistive heaters and a three-mode controller in ∼5 min. The cell was then pressurized to 50 atm from a small H_2 reservoir while stirring with a Teflon-coated stir bar in order to initiate the reaction. The pressure inside the reactor was followed via Honeywell atomic pressure transducer (Model TJE). For each set of experiments, a new reactor was used to avoid the possibility of contamination by metallic rhodium or rhodium complexes remaining from previous run.

■ ASSOCIATED CONTENT

Ⓢ Supporting Information. GC-MS investigation details and results of the hydrogenated Cp* products (Table SI-1); Hg(0) poisoning when one-third of the reaction was completed (Figure SI-1); GC-MS isotope distribution analysis of the resultant and comparison with the theoretical isotope distribution (Figure SI-2); EXAFS comparison of the CSU vs PNNL standard conditions (Figure SI-3); plots of hydrogenation reaction data and fits to a polynomial to calculate the order with respect to fully evolved Rh_{Total} catalyst (Figure SI-4); initial rate with respect to $[Rh_{Total}]^2$ and $[Rh_{Total}]^{1/2}$ concentrations graphs (Figure SI-5); TEM of the $Rh(0)_n$ nanoparticles at the end of the benzene hydrogenation reaction (Figure SI-6); benzene hydrogenation curve, its polynomial fit, and equation when starting with 50-fold lower concentration $Rh(0)_n$ nanoparticles (Figure SI-7); plots of hydrogenation reaction data and fits to a polynomial for 1,10-phenanthroline poisoning of Rh_4 clusters (Figure SI-8); and plots of hydrogenation reaction data and fits to a polynomial for 1,10-phenanthroline poisoning of authentic $Rh(0)_n$ nanoparticles (Figure SI-9). This material is free of charge via the Internet at http://pubs.acs.org.

■ AUTHOR INFORMATION

Corresponding Author
rfinke@lamar.colostate.edu; john.linehan@pnl.gov

■ ACKNOWLEDGMENT

■ REFERENCES

(1) (a) Schwartz's more modern definition[1b] of homogeneous vs heterogeneous catalysts is used herein (and in place of the older, historical definitions that equate "homogeneous" with soluble and "heterogeneous" with insoluble); see Figure 6 elsewhere.[9b] That is, homogeneity or heterogeneity of the catalyst is defined and used herein according to the catalytically active site(s): a homogeneous catalyst has a single, uniform catalyst site, whereas a heterogeneous catalyst has more than one active site. Hence, the catalytically active species uncovered herein, of Rh_4 clusters with the average stoichiometry of $Rh_4Cp*_{2.4}Cl_4H_c$, will be classified (admittedly a bit arbitrarily) as a homogeneous catalyst, since a single active site per each Rh_4 cluster is expected given the presence of bulky Cp* and Cl^- (and possibly H^-) ligands and since there is no evidence for more than a single active site within each Rh_4 cluster. This assignment should be considered tentative, especially since the evidence to follow will indicate the presence of more than one, on average, Rh_4 cluster in the evolved, "homogeneous" Rh_4 catalyst. (b) Schwartz, J. *Acc. Chem. Res.* **1985**, *18*, 302.

(2) Widegren, J. A.; Finke, R. G. *J. Mol. Catal. A: Chem.* **2003**, *198*, 317.

(3) Hagen, C. M.; Vieille-Petit, L.; Laurenczy, G.; Süss-Fink, G.; Finke, R. G. *Organometallics* **2005**, *24*, 1819.

(4) (a) Fulton, J. L.; Linehan, J. C.; Autrey, T.; Balasubramanian, M.; Chen, Y.; Szymczak, N. K. *J. Am. Chem. Soc.* **2007**, *129*, 11936. (b) Rousseau, R. J.; Schenter, G. K.; Fulton, J. L.; Linehan, J. C.; Engelthard, M. H.; Autrey, T. *J. Am. Chem. Soc.* **2009**, *131*, 10516–10524.

(5) Alley, W. M.; Hamdemir, I. K.; Wang, Q.; Frenkel, A. I.; Li, L.; Yang, J. C.; Menard, L. D.; Nuzzo, R. G.; Özkar, S.; Johnson, K. A.; Finke, R. G. *Inorg. Chem.* **2010**, *49*, 8131.

(6) Alley, W. M.; Hamdemir, I. K.; Wang, Q.; Frenkel, A. I.; Li, L.; Yang, J. C.; Menard, L. D.; Nuzzo, R. G.; Özkar, S.; Yih, K.-H.; Johnson, K. A.; Finke, R. G. *Langmuir* **2011**, *27*, 6279.

(7) (a) Uzun, A.; Gates, B. C. *Angew. Chem., Int. Ed.* **2008**, *47*, 9245. (b) Uzun, A.; Gates, B. C. *J. Am. Chem. Soc.* **2009**, *131*, 15887.

(8) Lin, Y.; Finke, R. G. *Inorg. Chem.* **1994**, *33*, 4891.

(9) (a) Lin, Y.; Finke, R. G. *J. Am. Chem. Soc.* **1994**, *116*, 8335. (b) Aiken, J. D., III; Lin, Y.; Finke, R. G. *J. Mol. Catal. A: Chem.* **1996**, *114*, 29. (c) Weiner, H.; Trovarelli, A.; Finke, R. G. *J. Mol. Catal. A: Chem.* **2003**, *191*, 253. (d) Hornstein, B. J.; Finke, R. G. *Chem. Mater.* **2003**, *15*, 899.

(10) Noteworthy here is that much of the basis for this underlying approach, for distinguishing homogeneous from heterogeneous catalysts, can in essence be traced back to seminal kinetic and mechanistic studies by J. Halpern and co-workers, even though distinguishing polymetallic from monometallic catalysts was not part of the following work: (a) Halpern, J. *Inorg. Chim. Acta* **1981**, *50*, 11. (b) Halpern, J.; Okamoto, T.; Zakhariev, A. *J. Mol. Catal.* **1977**, *2*, 65. (c) Landis, C. R.; Halpern, J. *J. Am. Chem. Soc.* **1987**, *109*, 1746.

(11) Alley, W. M.; Hamdemir, I. K.; Johnson, K. A.; Finke, R. G. *J. Mol. Catal. A: Chem.* **2010**, *315*, 1.

(12) *In operando* spectroscopy as used herein refers to any technique in which the catalyst is present in the reaction solvent at the operating temperature and pressure and also under the working conditions of the reactants and resultant products of that operating catalytic system: Tinnemans, S. J.; Mesu, J. G.; Kervinen, K.; Visser, T.; Nijhuis, T. A.; Beale, A. M.; Keller, D. E.; van der Eerden, A. M. J.; Weckhuysen, B. M. *Catal. Today* **2006**, *113*, 3.

(13) Platt, J. R. *Science* **1964**, *146*, 347.

(14) Widegren, J. A.; Finke, R. G. *J. Mol. Catal. A: Chem.* **2003**, *191*, 187.

(15) Gómez, M.; Favier, I. Metal Nanoparticles Dispersed in Solution: Tests to Identify the Catalyst Nature. In *Metal Nanoclusters in Catalysis and Materials Science: The Issue of Size Control*; Corain, B.,

18901

dx.doi.org/10.1021/ja2073438 |*J. Am. Chem. Soc.* 2011, 133, 18889–18902

Schmid, G., Toshima, N., Eds.; Elsevier: Amsterdam, The Netherlands, 2008; Ch. 31, pp 427−436.

(16) Bayram, E.; Zahmakıran, M.; Özkar, S.; Finke, R. G. *Langmuir* **2010**, *26*, 12455.

(17) Hornstein, B. J.; Aiken, J. D., III; Finke, R. G. *Inorg. Chem.* **2002**, *41*, 1625.

(18) Phan, N. T. S.; Sluys, M. V. D.; Jones, C. W. *Adv. Synth. Catal.* **2006**, *348*, 609.

(19) de Vries, J. G. *Dalton Trans.* **2006**, 421.

(20) Huang, L.; Ang, T. P.; Wang, Z.; Tan, J.; Chen, J.; Wong, P. K. *Inorg. Chem.* **2011**, *50*, 2094.

(21) Reimann, S.; Stötzel, J.; Frahm, R.; Kleist, W.; Grunwaldt, J.-D.; Baiker, A. *J. Am. Chem. Soc.* **2011**, *133*, 3921.

(22) Durand, J.; Teuma, E.; Gómez, M. *Eur. J. Inorg. Chem.* **2008**, 3577.

(23) Dyson, P. J. *Dalton Trans.* **2003**, 2964.

(24) Arpe, H. J.; Weissermel, K. *Industrial Organic Chemistry*, 4th ed.; Wiley-VCH: New York, 2003.

(25) Schulz, J.; Patin, H.; Roucoux, A. *Chem. Rev.* **2002**, *102*, 3757.

(26) Russell, M. J.; White, C.; Maitlis, P. M. *J. Chem. Soc. Chem. Commun.* **1977**, 427.

(27) Hagen, C. M.; Widegren, J. A.; Maitlis, P. M.; Finke, R. G. *J. Am. Chem. Soc.* **2005**, *127*, 4423.

(28) Collman, J. P.; Kosydar, K. M.; Bressan, M.; Lamanna, W.; Garrett, T. *J. Am. Chem. Soc.* **1984**, *106*, 2569.

(29) (a) Espinet, P.; Bailey, P. M.; Piraino, P.; Maitlis, P. M. *Inorg. Chem.* **1979**, *18*, 2706. (b) Maitlis, P. M. *Acc. Chem. Res.* **1978**, *11*, 301.

(30) (a) Watzky, M. A.; Finke, R. G. *J. Am. Chem. Soc.* **1997**, *119*, 10382 and references therein;. (b) Watzky, M. A.; Finke, R. G. *Chem. Mater.* **1997**, *9*, 3083. (c) Aiken, J. D., III; Finke, R. G. *J. Am. Chem. Soc.* **1998**, *120*, 9545 and references therein;. (d) Widegren, J. A.; Aiken, J. D., III; Özkar, S.; Finke, R. G. *Chem. Mater.* **2001**, *13*, 312 and references therein.

(31) Widegren, J. A.; Bennett, M. A.; Finke, R. G. *J. Am. Chem. Soc.* **2003**, *125*, 10301.

(32) (a) Jaska, C. A.; Temple, K.; Lough, A. J.; Manners, I. *J. Am. Chem. Soc.* **2003**, *125*, 9424. (b) Jaska, C. A.; Manners, I. *J. Am. Chem. Soc.* **2004**, *126*, 9776.

(33) Although the initial study[4a] suggested an equilibrium between Rh$_4$ and Rh$_6$ clusters and the true catalyst was suggested to be Rh$_{4-6}$ clusters, later ab initio molecular dynamics calculations[4b] suggest that the equilibrium is actually between tetrahedral and butterfly shaped Rh$_4$ clusters; see Figure 3 elsewhere.[4b]

(34) Staubitz, A.; Robertson, A. P. M.; Sloan, M. E.; Manners, I. *Chem. Rev.* **2010**, *110*, 4023.

(35) Senior, W. A.; Verrall, R. E. *J. Phys. Chem.* **1969**, *73*, 4242.

(36) Stern, E. A.; Newville, M.; Ravel, B.; Yacoby, Y. *Physica B* **1995**, *208&209*, 117.

(37) For low coordination numbers (<6), accurate measurements for the first coordination shell are possible with small uncertainties by XAFS. When coordination numbers approach 12, the precision of the size measurement greatly diminishes.[4,37a] (a) Frenkel, A. I.; Hills, C. W.; Nuzzo, R. G. *J. Phys. Chem. B* **2001**, *105*, 12689.

(38) Churchill, M. R.; Julis, S. A.; Rotella, F. J. *Inorg. Chem.* **1977**, *16*, 1137.

(39) Farrugia, L. J. *J. Cluster Sci.* **2000**, *11*, 39.

(40) Maitlis and co-workers found two different Rh−Rh bond lengths for [RhCp*H]$_4$[BF$_4$]$_2$ (2.610 and 2.829 Å) in which four hydrides are face bridging.[40a] This observation was explained via two different oxidation states of the rhodium atoms in the Rh$_4$ cluster (i.e., two Rh^{II} and two Rh^{III} per Rh$_4$ cluster). Our XAFS investigation shows that all Rh−Rh average bond lengths are equal; hence, any hydride ligands present would have to be consistent with this fact (e.g., four face-bridging hydrides or something else that makes the average Rh−Rh bond lengths equal). (a) Ricci, J. S.; Koetzle, T. F.; Goodfellow, R. J.; Espinet, P.; Maitlis, P. M. *Inorg. Chem.* **1984**, *23*, 1828.

(41) XPS analysis was performed using a Physical Electronics 5800 spectrometer equipped with a hemispherical analyzer and using monochromatic Al-Kα radiation (1486.6 eV, the X-ray tube working at 15 kV and 350 W) and a pass energy of 23.5 eV. The obtained binding

energies are consistent with the metallic rhodium binding energies (given in paranthesis): 307.03 eV (307.0 eV) for Rh 3d$_{5/2}$ and 311.7 eV (312.0 eV) for Rh 3d$_{3/2}$. (a) Moulder, J. F.; Stickle, W. F.; Sobol, P. E.; Bomben, K. D. *Handbook of X-ray Photoelectron Spectroscopy*; Physical Electronics, Inc.: Eden Prairie, MN, 1995.

(42) Wilkins, R. G. *Kinetics and Mechanisms of Reactions of Transition Metal Complexes*, 2nd ed.; VCH: New York, 1991.

(43) The number of metal atoms, y, per nth shell, in full shell "magic number" nanoparticles is given by the equation $y = 10n^2 + 2$ ($n > 0$). See Schmid, G. *Endeavour* **1990**, *14*, 172.

(44) The stoichiometry for the Standard Conditions Benzene Hydrogenation with [RhCp*Cl$_2$]$_2$ requires the use of excess ($\sim$15 equiv per total Rh) of Et$_3$N to scavenge the formed HCl from the precursor, [RhCp*Cl$_2$]$_2$. Because the experiments starting with the authentic, preformed Rh(0)$_n$ nanoparticles do not evolve HCl, no Et$_3$N was added for those benzene hydrogenation reactions. In addition, a separate control experiment with the authentic Rh(0)$_n$ nanoparticles [in which 14 equiv (per total Rh) of Et$_3$N plus 1 equiv (per total Rh) of Et$_3$N$^+$Cl$^-$ was added] yielded the same activity within experimental error as when Et$_3$N plus Et$_3$N$^+$Cl$^-$ were absent. The normal amount of 2-propanol (36 mL) and benzene (4 mL), as in the case of starting with [RhCp*Cl$_2$]$_2$, were used in these experiments.

(45) Of interest here is how the "catch 22" issue noted in our 1994 paper[8] (see Figure 4 elsewhere[8]) again appears in the present study. As Figure 4 elsewhere emphasizes,[8] what one ideally needs when attempting to identify the true catalyst in any reaction is authentic samples of each of the possible, proposed true catalysts for use in control experiments to determine everything from their relative catalytic activities, spectroscopic properties to their stabilities, solubilities, whether they can be removed by filtration or centrifugation and so on. But the problem is that these are often the same (putative; unknown) catalyst(s) that one is trying to identify in the first place and for the first time! A specific example here is the need, ideally, in the present studies for the putative Rh(0)$_n$ nanoparticles that could be present in the current system, nanoparticles that would then have a previously unknown set of surface ligands made up from the possible Cp*, Cl, H, benzene, Et$_3$N, and other possible ligands present in the system. Such a catalyst does not exist in the literature. That fact, however, does not mean it has not been made in the current benzene hydrogenation system and at a level ≤2%. The reader interested in solving more difficult cases of "what is the true catalyst?" will want to study Figure 4 elsewhere and the "catch 22" implication noted therein.

(46) Noteworthy here is that poisoning experiments with ligands, such as CS$_2$, PPh$_3$, and thiophene, are not expected to always be useful in cases, such as the present higher temperature benzene reduction catalysis, since their exothermic binding and insufficiently strong binding constants tend to cause these ligands to dissociate above 50 °C.[2] That said, it should be possible to find and develop other, polydentate poisons analogous to 1,10-phenanthroline as needed for future quantitative poisoning studies aimed at distinguishing single metal from polymetallic catalysts.

(47) Maxted, E. B. *Adv. Catal.* **1951**, *3*, 129.

(48) One alternative hypothesis that we can think of is that if the 1,10-phenanthroline binding constant of the Rh$_4$ clusters was orders of magnitude larger than the binding constant of the Rh(0)$_n$ nanoparticles, then it would be conceivable that all the added 1,10-phenanthroline poison could be bound first by the Rh$_4$ clusters, with no poisoning reaching the (in this case hypothesized, true) Rh(0)$_n$ catalyst until the 1,10-phenanthroline binding capacity of the Rh$_4$ clusters had been saturated. While both less consistent with the observed binding curves (as argued in the text) as well as physically unlikely, we believe, this possibility is being investigated via a more detailed, quantitative model and mechanistic analysis of the poisoning data designed to uncover the relative 1,10-phenanthroline binding constants of the Rh$_4$ and Rh(0)$_n$ catalysts. A preliminary quantitative analysis as part of that work supports what the curves themselves already suggest, namely, that if anything, the 1,10-phenanthroline binding constant for the Rh$_4$ appears to be smaller, not larger, than that for the Rh(0)$_n$ nanoparticles.